LOW-ENERGY SCATTERING ON THE LATTICE

DISSERTATION

ZUR

ERLANGUNG DES DOKTORGERADES (DR. RER. NAT.)

DER

MATHEMATISCH-NATURWISSENSCHAFTLICHEN FAKULTÄT

DER

RHEINISCHEN-FRIEDRICH-WILHELMS-UNIVERSITÄT

VORGELEGT VON

SHAHIN BOUR BOUR

AUS

TEHERAN

BONN MÄRZ 2014

Angefertigt mit Genehmigung der Mathematisch-Naturwissenschaftlichen Fakultät der Rheinischen Friedrich-Wilhelms-Universität Bonn

1. Referent: Prof. Ulf -G. Meißner

2. Referent: Prof. Hans -W. Hammer

Tag der Promotion: June 10, 2014

Erscheinungsjahr: 2014

Abstract

In this thesis we present precision benchmark calculations for two-component fermions in the unitarity limit using an *ab initio* method, namely Hamiltonian lattice formalism. We calculate the ground state energy for unpolarized four particles (Fermi gas) in a periodic cube as a fraction of the ground state energy of the non-interacting system for two independent representations of the lattice Hamiltonians. We obtain the values 0.211(2) and 0.210(2). These results are in full agreement with the Euclidean lattice and fixed-node diffusion Monte Carlo calculations. We also give an expression for the energy corrections to the binding energy of a bound state in a moving frame. These corrections contain informations about the mass and number of the constituents and are topological in origin and will have a broad applications to the lattice calculations of nucleons, nuclei, hadronic molecules and cold atoms. As one of its applications we use this expression and determine the low-energy parameters for the fermion dimer elastic scattering in shallow binding limit. For our lattice calculations we use Lüscher's finite volume method. From the lattice calculations we find $\kappa a_{\rm fd} = 1.174(9)$ and $\kappa r_{\rm fd} = -0.029(13)$, where κ represents the binding momentum of dimer and $a_{\rm fd}$ ($r_{\rm fd}$) denotes the scattering length (effective-range). These results are confirmed by the continuum calculations using the Skorniakov-Ter-Martirosian integral equation which gives 1.17907(1) and $-0.0383(3)$ for the scattering length and effective range, respectively. Both results for the fermion dimer effective range are not in agreement with the previous calculation [86] which have found $\kappa r_{\rm fd} \approx 0.08(1)$.

Acknowledgments

First, I would like to thank my advisor Prof. Ulf -G. Meißner for giving me the opportunity to work on this interesting matter and encouraging supervision.

My special gratitude is assigned to Prof. Hans -W. Hammer for shairing his analytic insight into and foundational experience with the subject of this thesis.

I would like to express the deepest appreciation to Prof. Dean J. Lee who always had a sympathic ear to answer arising questions and to find the appropriate words, when I was confused.

Thank is due to my office colleagues for the nice and simulating atmosphere at work, but also in non-academic circumstances.

I also would like to thank Matthias Frink, Dr. Mark Lenkewitz, Dr. Michael Lage and Dr. Domenik Hoja for always helping when it was needed. Thanks for the great time go to all members of the theory group of the "Helmholtz-Institut für Strahlen und Kernphysik".

Last but not the least, I want to thanks my Kamila who spent sleepless nights with and was always my support in the moments when there was no one to answer my queries.

Contributions in peer-reviewed journals

1. S. Bour, X. Li, D. Lee, U.-G. Meißner and L. Mitas,

   "Precision benchmark calculations for four particles at unitarity,"

   Phys. Rev. A **83** (2011) 063619.

2. S. Bour, S. König, D. Lee, H.-W. Hammer and U.-G. Meißner,

   "Topological phases for bound states moving in a finite volume,"

   Phys. Rev. D **84** (2011) 091503.

3. S. Bour, H.-W. Hammer, D. Lee and U.-G. Meißner,

   "Benchmark calculations for elastic fermion-dimer scattering,"

   Phys. Rev. C **86** (2012) 034003.

Contents

Chapter 1

Overview

1.1 Standard model

The standard model (SM) unifies three of four forces of nature. The SM is a local gauge theory with the gauge group $SU(3) \times SU(2) \times U(1)$ specifying the interactions among the basic constituents of matter. These basic constituents (see figure 1.1) are six *quarks*, each in three colors, and six *leptons*. The quarks and leptons are classified into three generations. The interactions between the particles are mediated by vector bosons; 8 *gluons* mediate the strong interactions, $W^{\pm}$ and Z mediate the weak interaction, and the electromagnetic interaction is transmitted by the photon γ. The weak bosons become massive through the *Higgs mechanism*.

1.2 Strong interactions

The strong interactions between the elementary particles are described by quantum chromodynamics (QCD). At the fundamental level, this is the gauge interaction based on the $SU(3)_c$ color group, which is a part of the gauge group $SU(3) \times SU(2) \times U(1)$ of the SM [1,2]. The Lagrangian of QCD (without gauge fixing and CP-violating term) is given by

$$\mathcal{L} = \bar{\psi}_i \big[i(\gamma^\mu \mathcal{D}_\mu)_{ij} - m\delta_{ij} \big] \psi_j - \frac{1}{4} \mathcal{G}^{a\mu\nu} \mathcal{G}^a_{\mu\nu}, \tag{1.1}$$

where the $\psi_i(x)$ are the quark fields in the fundamental representation of the $SU(3)$ gauge group, indexed by $i, j, \ldots$ and these indices are summed over. The covariant derivative is given by $\mathcal{D}_\mu = \partial_\mu - ig\tau^a \mathcal{G}^a_\mu$, where g is the coupling constant of the strong interaction

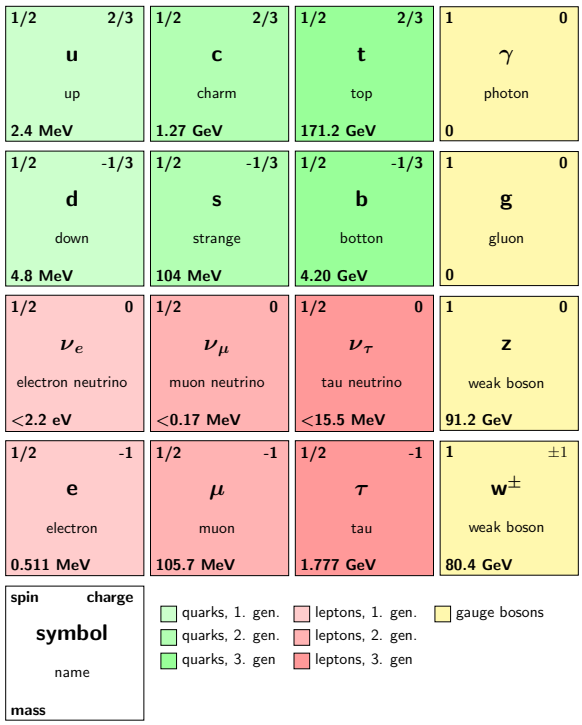

Figure 1.1: Basic constituents of matter.

and τ^a, which obey $\left[\tau^a, \tau^b\right] = if^{abc}\tau^c$, are the independent generators of the $SU(3)_c$ symmetry. $\mathcal{G}^a_{\mu\nu}$, represents the gauge invariant gluonic field strength tensor and is defined by $\left[\mathcal{D}_\mu, \mathcal{D}_\nu\right] = -ig\tau^a\mathcal{G}^a_{\mu\nu}$ or more explicitly, $\mathcal{G}^a_{\mu\nu} = \partial_\mu\mathcal{G}^a_\nu - \partial_\nu\mathcal{G}^a_\mu - gf^{abc}\mathcal{G}^b_\mu\mathcal{G}^c_\nu$, where $\mathcal{G}^a_\mu$ are the gluon fields in the adjoint representation of the $SU(3)$ gauge group, indexed by $a, b, \ldots$ and f^{abc} are the structure constants of $SU(3)$. QCD is an asymptotically free theory which means the coupling constant of QCD decreases at higher energies as we can see in figure 1.2. This weakness of the interactions allows one to apply perturbative calculations at high energies. However at low energies the strong interaction becomes stronger, and perturbation theory is no longer applicable. To deal with this problem one can use the *effective field theory* technique or *non-perturbative* methods like *lattice* QCD.

1.3 Effective field theories

An astonishing fact about the world we live in is the existence of interesting physics at all scales. From the size of the universe to the size of nucleons, we can find fascinating

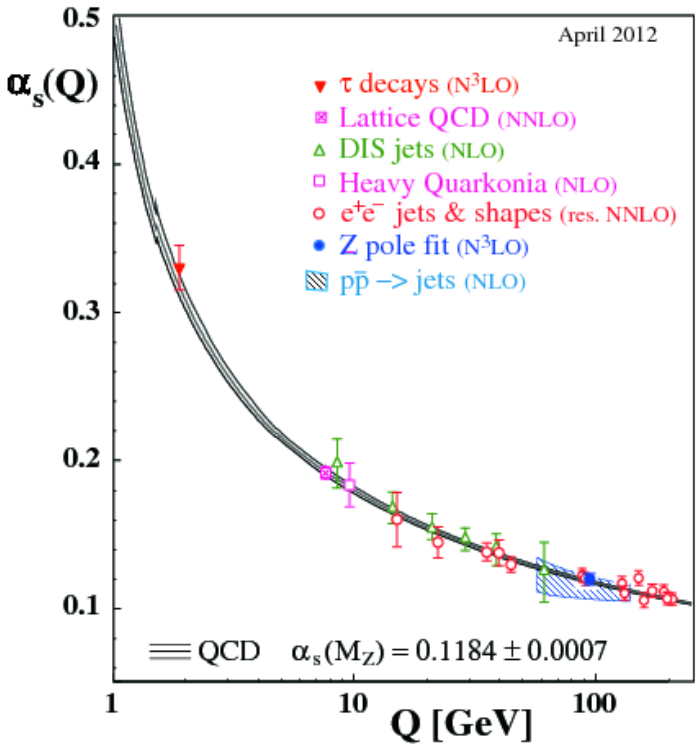

Figure 1.2: Summary of measurements of α_s as a function of the respective energy scale Q. The respective degree of QCD perturbation theory used in the extraction of α_s is indicated in brackets (NLO: next-to-leading order; NNLO: next-to-next-to leading order; res. NNLO:NNLO matched with resummed next-to-leading logs; N3LO: next-to-NNLO). Picture from [3]

physical phenomena. The effective field theory (EFT) idea emanates from this fact that scales much bigger or smaller than the ones we are interested in do not affect the dynamics of the system in question too strongly [4–6]. This fact might be one of the reasons why two revolutionary ideas in physics, *quantum mechanics* and *relativity*, did not come earlier since the quantum mechanics and relativity are relevant in very tiny and large distances, respectively. Lets make the idea of EFT more clear by an example. Assume we have a theory with a set of light and heavy fields, their respective masses well separated by a scale Λ. In the low-energy regime, which means energies well below Λ, the heavy degrees of freedom can be integrated out of the generating functional. What remains is an effective Lagrangian with only light degrees of freedom. This procedure can produce a non-renormalizable theory. To build an effective theory we need to choose the suitable degrees of freedom. We can construct the Lagrangian based on the symmetries of the fundamental theory. Certainly an effective

theory must be consistent with the full theory and experiments. In other words since the only content of quantum field theory (QFT) are *unitarity*, *analyticity*, *cluster decomposition* and *symmetries*, to build an effective Lagrangian one must take the most general Lagrangian, which contains these principles [7]. Two examples of effective theories are Fermi's theory of beta decay (weak interaction) and chiral perturbation theory (QCD).

Any EFT builds on a basic physics principle that underlies every low-energy effective model or theory. A high-energy, short-wavelength probe sees details down to scales comparable to the wavelength. Thus, electron scattering at sufficiently high energy reveals the quark substructure of protons and neutrons in a nucleus. But at lower energies, details are not resolved, and one can replace short-distance structure with something simpler, as in a multipole expansion of a complicated charge or current distribution. This means it is not necessary to calculate with full QCD to do accurate strong interaction physics at low energies; we can replace quarks and gluons by neutrons and protons (and maybe pions and ...). EFT provides a systematic, model-independent way to carry out this program starting with a local Lagrangian framework.

An EFT is formulated by specifying appropriate low-energy degrees of freedom and then constructing the Lagrangian as a complete set of terms that embody the symmetries of the underlying theory. There is not a unique EFT for nuclear physics. In different applications the relevant degrees of freedom might be neutrons and protons only, or neutrons, protons, and pions, or neutrons, protons, pions, and Δ's or quasi-nucleons [13]. The form of the EFT can be chosen to readily expose universal behavior, such as features in *dilute neutron matter* that are common with phenomena seen in *cold atom* experiments. We will come back to this later on. In applying an EFT Lagrangian, one must confront in a controlled way the impact of excluded short-distance physics. Quantum mechanics implies that sensitivity to short-distance physics is always present in a low-energy theory, but it is made manifest in an EFT through the dependence on a cutoff or other regulator instead of being hidden in phenomenological form factors. Removing this dependence necessitates a well-defined regularization and renormalization scheme as part of the EFT. This necessity becomes a virtue as residual regulator dependence can be used to assess truncation errors and many-body approximations. Furthermore, the freedom in how to regulate coupled with the freedom to make unitary transformations can be exploited by renormalization group methods to greatly simplify few- and many-body nuclear calculations.

For an EFT calculation to be improvable order-by-order, one needs a scheme to

organize the infinity of possible terms in the Lagrangian based on an expansion parameter. Such a scheme is called a power counting. Power counting tells us what terms (or Feynman diagrams) to include at each order and lets us estimate the theoretical truncation error. The radius of convergence associated with the expansion means that the EFT predicts it own downfall, in contrast to phenomenological models. EFT expansion parameters most commonly arise as a ratio of disparate physical scales rather than as a small coupling constant (e.g., as in Coulomb systems); a many-body example is the ratio of the range of the interaction to the interparticle spacing in a dilute system. The power counting for this example is particularly simple when the scattering length is roughly the same size as the interaction range (called "natural") but changes dramatically if the scattering length is much larger (called "unnatural"). In the following we give a brief overview of the concept of the scattering length and the effective range expansion and the application of EFT to cold atoms.

1.3.1 Scattering length and effective range expansion

The scattering length is one of the central observables in nuclear physics. The concept of the scattering length is introduced in every graduate quantum mechanics course. Here we will briefly reintroduce this quantity [16, 17]. Consider a system of two identical particles moving in their center-of-mass system with momentum $\mathbf{p}$. The asymptotic wave function is of the form

$$\Psi \sim e^{i\mathbf{p}\cdot\mathbf{r}} + \mathcal{A}(p,\theta)\frac{e^{ipr}}{r}, \tag{1.2}$$

where θ represents the scattering angle and p and r denote $|\mathbf{p}|$ and $|\mathbf{r}|$, respectively. This wave function is the superposition of an incident plane wave and a scattered wave function. In Eq. (1.2), $\mathcal{A}(p,\theta)$ is called the scattering amplitude and is related to the differential cross-section via

$$\frac{d\sigma}{d\Omega} = |\mathcal{A}(p,\theta)|^2. \tag{1.3}$$

The scattering amplitude can be written as a sum of contributions from different partial waves

$$\mathcal{A}(p,\theta) = \frac{1}{2ip}\sum_{l=0}^{\infty}(2l+1)\big(e^{2i\delta_l}-1\big)P_l(\cos\theta), \tag{1.4}$$

where $P_l(\cos\theta)$ denote the Legendre polynomials and δ_l is the scattering phase shift. The partial wave amplitude can be defined as

$$\mathcal{A}_l(p,\theta) = \frac{e^{2i\delta_l(p)}-1}{2ip}, \tag{1.5}$$

which can be written as

$$\mathcal{A}_l(p,\theta) = \frac{1}{p\cot\delta_l - ip}. \tag{1.6}$$

At very low energies the cross-section for 2-body scattering is dominated by the S-wave amplitude. The higher partial waves are suppressed by powers of the relative momentum. The S-wave scattering amplitude for two particles with relative momentum p is

$$\mathcal{A}_0(p) = \frac{1}{p\cot\delta_0 - ip}, \tag{1.7}$$

where δ_0 is the S-wave phase shift. At low momentum the S-wave phase shift for 2-body scattering with short-range interactions can be characterized in terms of the effective range expansion,

$$p\cot\delta_0 = -\frac{1}{a_{\rm s}} + \frac{1}{2}r_{\rm eff}\,p^2 + \cdots . \tag{1.8}$$

Here, $a_{\rm s}$ is the S-wave scattering length, and $r_{\rm eff}$ is the S-wave effective range. The radius of convergence of the effective range expansion is controlled by the characteristic length scale of the interaction. For example in low-energy nuclear physics the range of the two-nucleon interaction is set by the Compton wavelength of the pion.

1.3.2 Effective field theory for cold atoms at unitarity

The EFT for the unitarity limit can be derived from any theory of two-component fermions with infinite scattering length and negligible higher-order scattering effects at the relevant low-momentum scale. For example the two fermion components may correspond to dressed hyperfine states $\left|F,m_F\right\rangle = \left|9/2,-9/2\right\rangle$ and $\left|9/2,-7/2\right\rangle$ of ^{40}K with interactions given either by a full multi-channel Hamiltonian or a simplified two-channel model. We should remind that the hyperfine levels of an atom are labeled by the set of quantum numbers (F, m_F). Here F is the quantum number for the total angular momentum of the atom. The total angular momentum, $\mathbf{F}$ is given by

$$\mathbf{F} = \mathbf{J} + \mathbf{I} = \mathbf{L} + \mathbf{S} + \mathbf{I}, \tag{1.9}$$

where $\mathbf{L}$ represents the sum of the electronic angular momenta, $\mathbf{S}$ denotes the sum of the electronic spins and $\mathbf{I}$ is the nuclear spin. m_F is the quantum number of the third component of the total angular momentum.

The starting point to drive the EFT for the unitarity limit does not matter so long as the S-wave scattering length is tuned to infinity to produce a zero-energy resonance. In

this work m represents the atomic mass and a_i and $a_i^\dagger$ are annihilation and creation operators for two hyperfine states. We label these as up and down spins, $i =\uparrow,\downarrow$, even though the connection with actual intrinsic spin is not necessary. The free non-relativistic effective Hamiltonian in momentum space can be written as

$$H_{\text{free}} = \sum_i \int d^3\vec{p}\ \frac{\vec{p}^{\,2}}{2m}\ a_i^\dagger(\vec{p}) a_i(\vec{p}). \tag{1.10}$$

In position space the annihilation and creation operators can be expressed as

$$a_i(\vec{r}) = \frac{1}{\sqrt{V}} \int d^3\vec{p}\ e^{i\vec{p}\cdot\vec{r}} a_i(\vec{p}), \quad a_i^\dagger(\vec{r}) = \frac{1}{\sqrt{V}} \int d^3\vec{p}\ e^{-i\vec{p}\cdot\vec{r}} a_i^\dagger(\vec{p}). \tag{1.11}$$

Combining Eqs. (1.10) and (1.11) the free Hamiltonian in configuration space is then given by

$$\begin{aligned} H_{\text{free}} &= -\frac{1}{2m} \sum_i \int d^3\vec{r}\ a_i^\dagger(\vec{r}) \vec{\nabla}^2 a_i(\vec{r}) \\ &= \frac{1}{2m} \sum_i \int d^3\vec{r}\ \big(\vec{\nabla} a_i^\dagger(\vec{r})\big) \cdot \big(\vec{\nabla} a_i(\vec{r})\big). \end{aligned} \tag{1.12}$$

The effective potential can be written as

$$V(\vec{r},\vec{r}\,') = \frac{1}{2} \sum_{i,j=\uparrow,\downarrow} \int d^3\vec{r} \int d^3\vec{r}\,' : a_i^\dagger(\vec{r}) a_i(\vec{r}) \mathcal{V}(\vec{r}-\vec{r}\,') a_j^\dagger(\vec{r}\,') a_j(\vec{r}\,') :, \tag{1.13}$$

where $: \cdots :$ denotes normal ordering. The leading order (LO) potential can be achieved by

$$\mathcal{V}_{\text{LO}}(\vec{r}-\vec{r}\,') = C_0\ \delta(\vec{r}-\vec{r}\,'). \tag{1.14}$$

C_0 denotes the 2-body coupling constant and is directly related to the 2-body scattering length. The exact value of C_0 depends on the scheme used to regulate the short distance behavior in the effective theory. The effective Hamiltonian at LO is

$$H_{\text{LO}} = -\frac{1}{2m} \sum_i \int d^3\vec{r}\ a_i^\dagger(\vec{r}) \vec{\nabla}^2 a_i(\vec{r}) + \frac{C_0}{2} \sum_{i,j} \int d^3\vec{r}\ \ : a_i^\dagger(\vec{r}) a_i(\vec{r}) a_j^\dagger(\vec{r}) a_j(\vec{r}) : . \tag{1.15}$$

Higher-order effects may be introduced systematically as higher-dimensional local operators with more derivatives and/or more local fields.

1.4 Lattice QCD

Lattice QCD (LQCD) is a non-perturbative method to deal with QCD. It is a discrete gauge theory formulated on the lattice of points in space and time. One of the first questions

that might come to one's mind is why using a lattice, although all physical experiments show no deviation from the continuous symmetries of the Lorentz group? The primary goal of LQCD is to test if QCD is the correct theory of strong interaction. One of the best evidences that we have for confinement in non-Abelian gauge theory comes by the Wilson formulation of a gauge theory set up on a four-dimensional Euclidean lattice. The lattice provides a natural cutoff removing the ultraviolet infinities. The lattice eliminates all wavelengths less than twice the lattice spacing $a_{\rm latt}$, before any expansions or approximations and thus on a lattice, a field theory becomes mathematically well-defined. A lattice formulation emphasizes the close connections between field theory and statistical mechanics. Indeed, the strong coupling treatment is equivalent to a high temperature expansion. The deep ties between these disciplines are manifest in the Feynman path integral formulation of quantum mechanics. In Euclidean space, a path integral is equivalent to a partition function of an analogous statistical system. After a Wick rotation the phase in the path integral becomes an exponential damping factor. One of the advantages of lattice formulation of a gauge theory is that the path integral transforms into an ordinary multiple integral over the fields. The starting point of lattice calculation is the partition function in Euclidean space-time

$$\mathcal{Z} = \int \mathcal{D}A_\mu \; \mathcal{D}\bar{\psi} \; \mathcal{D}\psi \; e^{-S}, \tag{1.16}$$

where S is the QCD action and is given by

$$S = \int d^4x \big(\frac{1}{4} G_{\mu\nu} G^{\mu\nu} - \bar{\psi} M \psi\big), \tag{1.17}$$

and M is the Dirac operator. The Grassmann fermionic fields, ψ and $\bar{\psi}$, can be integrated out from Eq. (1.16) and will be contained in a highly non-local term ($\det M$),

$$\mathcal{Z} = \int \mathcal{D}A_\mu \;\; \det M \;\; e^{-\frac{1}{4}\int d^4x \;\; G_{\mu\nu} G^{\mu\nu}}. \tag{1.18}$$

So the partition function is an integral over only background gauge configurations. Results for physical observables can be obtained by calculating expectation values

$$\langle \mathcal{O} \rangle = \frac{1}{\mathcal{Z}} \int \mathcal{D}A_\mu \; \mathcal{O} \; e^{-S}, \tag{1.19}$$

where $\mathcal{O}$ is any given combination of operators expressed in terms of time-ordered products of gauge and quark fields. Now the question is, how to extract physical observables from the expectation values? The correlation function gives the amplitude for creating and annihilating

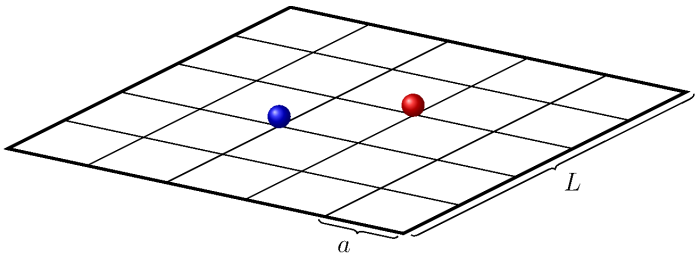

Figure 1.3: Two-dimensional-lattice

a state with definite quantum numbers between two points. The evaluation between these two points occurs via the QCD Hamiltonian. The physical observables can be extracted from the rate of the exponential fall-off in time and form the amplitude. There are three sources of uncertainty in LQCD. The first error source is coming from finite volume. The number of lattice points in the LQCD simulations are of course finite. The second one is caused by non-zero lattice spacing and the third source is non-physical quark masses. It is very difficult to go to the large boxes and make lattice spacing very small and take the physical quark masses. These limitations produce artifacts in the measurements of the LQCD which should be removed by extrapolations.

1.5 Effective field theory on the lattice

We discuss methods which combine EFT with lattice methods and which can be applied to both cold atomic systems and low-energy nuclear physics [26–30]. Unfortunately lattice QCD calculations of few- and many-body systems are at the present time hardly possible. Such simulations require pion masses at or near the physical mass and lattices several times longer in each dimension than used in current simulations. Another significant computational challenge is to overcome the exponentially small signal-to-noise ratio for simulations at large quark number. For few- and many-body systems in low-energy nuclear physics one can make further progress by working directly with hadronic degrees of freedom. Lattice effective field theory [28] provides an alternative method to describe few- and many-body systems at low energy without losing connection to QCD. In the lattice effective field theory approach we have effective field theory up to a given order in expansion parameter with lattice regularization. This approach uses low-energy scattering data as input and we can systematically improve the accuracy in describing low-energy phenomena by increasing

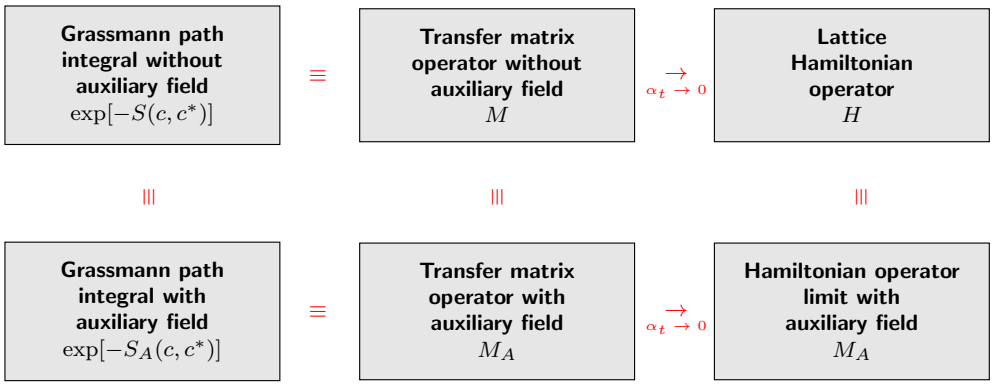

Figure 1.4: A schematic diagram of different lattice formulations. Using the Hubbard-Stratonovich-transformation 2-body problem can be transformed to the 1-body interacting with a background field (auxiliary field). Picture inspired by [26].

the order in power counting. In our discussion of the lattice formalism we use dimensionless parameters and operators corresponding with physical quantities multiplied by the appropriate power of the spatial lattice spacing a_{latt}. $\vec{n}$ denote spatial lattice points on a three-dimensional L^3 periodic cube and $\hat{\mu} = \hat{1}, \hat{2}, \hat{3}$ represent unit lattice vectors in the spatial directions. The temporal lattice spacing is denoted by a_t. We define α_t as the ratio of the lattice spacing, $\alpha_t = a_t/a_{\text{latt}}$. We also define $h = \alpha_t/(2m)$, where m is the fermion mass in lattice units. In the following we will introduce a number of different lattice formulations for a system of two-component fermions with attractive zero range interaction. These lattice formulations are shown schematically in 1.4. One can see in 1.4 that some of these formulations are equivalent or can merge to another.

1.5.1 Lattice regularization and Hamiltonian lattice formalism

At sufficiently low energies usually the short distance quantum structure of the particles is not important. Often the physical mass can be taken as input parameter to determine other physical observables like the energy spectrum. Assume we have one particle system on one spatial dimension of length L with periodic boundary condition. One of the physical observables which we are interested in is the energy spectrum. The energy in such systems is given by the following dispersion relation

$$E(p) = \sqrt{p^2 + m^2}, \quad p = \frac{2\pi}{L} n, \; n \in \mathbb{Z}, \tag{1.20}$$

where m is the physical mass of the particle and p is the one-dimensional momentum and is discrete. For low energies (energies much smaller than the mass m) the spectrum is given by

$$E(p) = m + \frac{p^2}{2m} + O(p^4). \tag{1.21}$$

The determination of the physical observables in more than the 1-body sector is usually followed by complications. Suppose we have a 2-body system on a one dimensional torus of length L. The non-interacting Hamiltonian in momentum space can be derived as

$$H_{\text{free}} = \sum_p \frac{p^2}{2m} a_p^\dagger a_p. \tag{1.22}$$

The interaction term can be defined through a delta-function potential. At low energies one can neglect the higher terms in the effective range expansion formula and so

$$p_{\text{cm}} \cot \delta_0(p_{\text{cm}}) \approx -\frac{1}{a}, \tag{1.23}$$

where p_{cm} represent the center-of-mass momentum. This allows us to take a contact interaction as the interaction term. In 2-body sector the general form of the potential is then given by

$$V = \frac{1}{2}\int_0^L dx_1 \int_0^L dx_2 : a^\dagger(x_1)a(x_1)V(x_1,x_2)a^\dagger(x_2)a(x_2) : . \tag{1.24}$$

By replacing $V(x_1, x_2)$ with a delta-function we will obtain

$$V = \frac{1}{2}C_0 \int_0^L dx : \big(a^\dagger(x)a(x)\big)^2 : . \tag{1.25}$$

In the momentum basis the annihilation and creation operators are defined as

$$a(x) = \frac{1}{\sqrt{L}} \sum_p e^{ipx} a_p, \quad a^\dagger(x) = \frac{1}{\sqrt{L}} \sum_p e^{-ipx} a_p^\dagger. \tag{1.26}$$

By replacing the annihilation and creation operators for momentum space in Eq. (1.25) we can find the interaction term in momentum space,

$$V = \frac{1}{2}\frac{C_0}{L} \sum_{p_1,p_2,p_1',p_2'} a_{p_1'}^\dagger a_{p_2'}^\dagger a_{p_2} a_{p_1} \ \delta_{p_1+p_2,p_1'+p_2'}, \tag{1.27}$$

where p_i and p_i' denote the momentum before and after the interaction. To find the physical observables for such systems we need to get rid of the ultraviolet divergences. One way to avoid them is to introduce a cutoff momentum, Λ. That means we will have $\Lambda L/\pi$

momentum modes ($p = 0, \pm\frac{2\pi}{L}, \pm\frac{4\pi}{L}, \cdots, \pm\Lambda$) which resulting $(\Lambda L/\pi)^3$ interaction terms. One should note that this number of interaction terms is just for one spatial dimension. In D spatial dimensions we will have $(\Lambda L/\pi)^{3D}$ interaction terms. As we can see the number of interaction terms depends on cutoff and volume. Through this dependence the number of terms can explode rapidly and this makes the computation expensive. The other way to avoid the divergences is to use lattice regularization. To discretize the space we use the following transformations

$$\begin{aligned}
&\int_0^L dx \to a_{\text{latt}} \sum_{n=0}^{N-1}, \\
&a(x) \to a(n), \quad n = 0, 1, \cdots, N-1, \quad a(N) = a(0), \\
&\frac{\partial}{\partial x} a(x) \to \frac{a(n+1) - a(n)}{a_{\text{latt}}} \quad \text{or} \quad \frac{a(n) - a(n-1)}{a_{\text{latt}}}, \\
&[a(n), a^\dagger(n)] = \delta_{n,n'}.
\end{aligned} \tag{1.28}$$

For a torus the lattice spacing is $a_{\text{latt}} = L/N$. The free Hamiltonian of the system in position space is

$$H_{\text{free}} = -\frac{1}{2m} \int_0^L dx \; a^\dagger(x) \frac{\partial^2}{\partial x^2} a(x) = \frac{1}{2m} \int_0^L dx \Big(\frac{\partial}{\partial x} a^\dagger(x) \Big) \Big(\frac{\partial}{\partial x} a(x) \Big). \tag{1.29}$$

The discretized non-interacting Hamiltonian is given by

$$H_{\text{free}} = -\frac{1}{2m} \sum_{n=0}^{N-1} \big[a^\dagger(n+1) a(n) + a^\dagger(n) a(n+1) - 2 a^\dagger(n) a(n) \big]. \tag{1.30}$$

It is easy to show that the energy spectrum of the free Hamiltonian is given by

$$E(p) = \frac{1}{m} \sum_i \big(1 - \cos p_i \big). \tag{1.31}$$

where i is the number of particles. In the 1-body sector we can immediately see that the energy spectrum which we find from the lattice method is the same as the energy spectrum found in Eq. (1.21)

$$\frac{1}{m} \big(1 - \cos p \big) = \frac{p^2}{2m} + O(p^4). \tag{1.32}$$

After including the interaction term we can find the lattice Hamiltonian of the system

$$H = H_{\text{free}} + \frac{C_0}{2} \sum_{n=0}^{N-1} : \big(a^\dagger(n) a(n) \big)^2 : . \tag{1.33}$$

For a system of two-component fermions the free lattice Hamiltonian on a three dimensional lattice can be written as

$$H_{\text{free}} = \frac{3}{m}\sum_{\vec{n},i} a_i^\dagger(\vec{n})a_i(\vec{n}) - \frac{1}{2m}\sum_{\vec{n},i}\sum_{\hat{\mu}=\hat{1},\hat{2},\hat{3}}\Big[a_i^\dagger(\vec{n})a_i(\vec{n}+\hat{\mu}) + a_i^\dagger(\vec{n})a_i(\vec{n}-\hat{\mu})\Big], \tag{1.34}$$

and so the interacting lattice Hamiltonian will be

$$H = H_{\text{free}} + \frac{C_0}{2}\sum_{\vec{n}} a_\uparrow^\dagger(\vec{n})a_\uparrow(\vec{n})a_\downarrow^\dagger(\vec{n})a_\downarrow(\vec{n}). \tag{1.35}$$

1.5.2 Grassmann path integral without auxiliary field

The simplest formulation to derive the Feynman rules is the lattice Grassmann path integral without auxiliary field [26]. Let c_i and c_i^* be anticommuting Grassmann fields for two-component fermions with spin up and down. These Grassmann fields are periodic with respect to the spatial lengths and antiperiodic along the temporal direction,

$$\begin{aligned} c_i(\vec{n}+L\hat{\mu},n_t) &= c_i(\vec{n},n_t), \qquad c_i^*(\vec{n}+L\hat{\mu},n_t) = c_i^*(\vec{n},n_t), \\ c_i(\vec{n},n_t+L_t) &= -c_i(\vec{n},n_t), \qquad c_i^*(\vec{n},n_t+Lt) = -c_i^*(\vec{n},n_t). \end{aligned} \tag{1.36}$$

The Grassmann path integral can be written as

$$\mathcal{Z} = \int \mathcal{D}c\mathcal{D}c^* \ \exp[-S(c,c^*)], \tag{1.37}$$

where the action and the measure of integral are given by

$$\begin{aligned} S(c,c^*) &= S_{\text{free}}(c,c^*) + C_0\alpha_t\sum_{\vec{n},n_t}\rho_\uparrow(\vec{n},n_t)\rho_\downarrow(\vec{n},n_t). \\ \mathcal{D}c\mathcal{D}c^* &= \prod_{\vec{n},n_t,i} dc_i(\vec{n},n_t)dc_i^*(\vec{n},n_t). \end{aligned} \tag{1.38}$$

The free, non-relativistic fermion action is

$$\begin{aligned} S_{\text{free}}(c,c^*) = &\sum_{\vec{n},n_t,i}\Big[c_i^*(\vec{n},n_t)c_i(\vec{n},n_t+1) - (1-6h)c_i^*(\vec{n},n_t)c_i(\vec{n},n_t)\Big] \\ &- h\sum_{\vec{n},n_t,i}\Big[c_i^*(\vec{n},n_t)c_i(\vec{n}+\hat{\mu},n_t) + c_i^*(\vec{n},n_t)c_i(\vec{n}-\hat{\mu},n_t)\Big]. \end{aligned} \tag{1.39}$$

The local Grassmann densities are defined in terms of bilinear products of the Grassmann fields,

$$\begin{aligned}\rho_\uparrow(\vec{n}, n_t) &= c^*_\uparrow(\vec{n}, n_t)c_\uparrow(\vec{n}, n_t),\\ \rho_\downarrow(\vec{n}, n_t) &= c^*_\downarrow(\vec{n}, n_t)c_\downarrow(\vec{n}, n_t),\\ \rho(\vec{n}, n_t) &= \rho_\uparrow(\vec{n}, n_t) + \rho_\downarrow(\vec{n}, n_t).\end{aligned} \tag{1.40}$$

The coefficient C_0 in Eq. (1.38) denotes the 2-body coupling constant and its exact value depends on the scheme used to regulate the short distance behavior.

1.5.3 Transfer matrix operator without auxiliary field

Assume the annihilation and creation operators of fermions satisfy the usual anti-commutation relations,

$$\begin{aligned}\{a, a^\dagger\} &= 1,\\ \{a, a\} = \{a^\dagger, a^\dagger\} &= 0.\end{aligned} \tag{1.41}$$

As we know there is an identity for any function $f(a^\dagger, a)$, which gives the relation between the Grassmann path integral and products of operators [31]. This identity is

$$\mathrm{Tr}\left[: f(a^\dagger, a) : \right] = \int dcdc^*\ e^{2c^*c} f[c^*, c], \tag{1.42}$$

where c and c^* are Grassmann variables and $: \cdots :$ indicates normal ordering. The trace in Eq. (1.42) is evaluated over all possible fermion states. Using the complete set of possible functions $\{1, a, a^\dagger, a^\dagger a\}$ we can immediately see the correctness of Eq. (1.42). One can rewrite Eq. (1.42) in a way that resembles a path integral over a short time interval with antiperiodic boundary condition,

$$\begin{aligned}\mathrm{Tr}\left[: f(a^\dagger, a) : \right] &= \int dc(0)dc^*(0)\ e^{c^*(0)[c(0)-c(1)]} f[c^*(0), c(0)],\\ c(1) &= -c(0).\end{aligned} \tag{1.43}$$

This result can be generalized for arbitrary numbers of operators. If $a_i(\vec{n})$ and $a_i^\dagger(\vec{n})$ represent fermion annihilation and creation operators for spin i at lattice site $\vec{n}$, we can rewrite any

Grassmann path integral as the trace of a product of operators by using the identity

$$\begin{aligned}
&\mathrm{Tr}\Big[: F_{L_t-1}\big[a^\dagger_{i'}(\vec{n}'), a_i(\vec{n})\big] : \times \cdots \times : F_0\big[a^\dagger_{i'}(\vec{n}'), a_i(\vec{n})\big] : \Big] \\
&= \int DcDc^* \ \exp\Big\{c^*_i(\vec{n}, n_t)\big[c_i(\vec{n}, n_t) - c_i(\vec{n}, n_t+1)\big]\Big\} \\
&\times \prod_{n_t=0}^{L_t-1} F_{n_t}\big[c^*_{i'}(\vec{n}', n_t), c_i(\vec{n}, n_t)\big],
\end{aligned} \tag{1.44}$$

with antiperiodic boundary condition,

$$c_i(\vec{n}, L_t) = -c_i(\vec{n}, 0). \tag{1.45}$$

To rewrite the path integral $\mathcal{Z}$, defined in Eq. (1.37) as a transfer matrix partition function, we use Eq. (1.34) and define the lattice density operators

$$\begin{aligned}
\rho^{a^\dagger a}_\uparrow(\vec{n}) &= a^\dagger_\uparrow(\vec{n}) a_\uparrow(\vec{n}), \\
\rho^{a^\dagger a}_\downarrow(\vec{n}) &= a^\dagger_\downarrow(\vec{n}) a_\downarrow(\vec{n}), \\
\rho^{a^\dagger a}(\vec{n}) &= \rho^{a^\dagger a}_\uparrow(\vec{n}) + \rho^{a^\dagger a}_\downarrow(\vec{n}).
\end{aligned} \tag{1.46}$$

After using Eq. (1.44) the transfer matrix partition function is,

$$\mathcal{Z} = \mathrm{Tr}\Big(M^{L_t}\Big), \tag{1.47}$$

where M is the normal-ordered transfer matrix operator and is given by

$$M =: \exp\Big[- H_{\mathrm{free}}\alpha_t - C_0\alpha_t \sum_{\vec{n}} \rho^{a^\dagger a}_\uparrow(\vec{n})\rho^{a^\dagger a}_\downarrow(\vec{n})\Big] : . \tag{1.48}$$

1.5.4 Grassmann path integral with auxiliary field

By coupling an auxiliary field to the particle density we can rewrite the Grassmann path integral. Due to the properties of the action such as simple contact interaction and anticommutiation of Grassmann variables, there is a large class of auxiliary-field transformations which let the action invariant. We consider a general auxiliary-field transformation A. Let us define the Grassmann action

$$S(c, c^*) = S_{\mathrm{free}}(c, c^*) - \sum_{\vec{n}, n_t} A[s(\vec{n}, n_t)] \cdot [\rho_\uparrow(\vec{n}, n_t) + \rho_\downarrow(\vec{n}, n_t)], \tag{1.49}$$

and the Grassmann path integral

$$\mathcal{Z} = \prod_{\vec{n},n_t} \Big[\int ds(\vec{n},n_t) \Big] \int DcDc^* \ \exp\big[-S(c,c^*,s)\big], \tag{1.50}$$

where s is real-valued over all lattice sites. If we define the auxiliary-field transformation so that

$$\begin{aligned} \int ds(\vec{n},n_t) 1 &= 1, \\ \int ds(\vec{n},n_t) A[s(\vec{n},n_t)] &= 0, \end{aligned} \tag{1.51}$$

we can factor out the term in Eq. (1.50) involving the auxiliary field s at $\vec{n},n_t$. We find

$$\begin{aligned} \int ds \ \exp\big[A(s)(\rho_\uparrow+\rho_\downarrow)\big] &= \int ds \ \big[1 + A(s)(\rho_\uparrow+\rho_\downarrow) + A^2(s)\rho_\uparrow\rho_\downarrow\big] \\ &= 1 + \int ds \ A^2(s)\rho_\uparrow\rho_\downarrow = \exp\Big[\int ds A^2(s)\rho_\uparrow\rho_\downarrow\Big]. \end{aligned} \tag{1.52}$$

Therefore the last condition needed to recover Eq. (1.37) is

$$-C_0\alpha_t = \int ds \ A^2(s). \tag{1.53}$$

1.5.5 Transfer matrix operator with auxiliary field

Using the exact formula in Eq. (1.44) we can write the Grassmann path integral $\mathcal{Z}$ as a product of transfer matrix operators that depend on the auxiliary fields

$$\mathcal{Z} = \prod_{\vec{n},n_t} \Big[\int ds(\vec{n},n_t) \Big] \operatorname{Tr}\{M(s,L_t-1)\cdots M(s,0)\}, \tag{1.54}$$

where

$$M(s,n_t) =: \exp\Big\{ -H_{\text{free}}\alpha_t + \sum_{\vec{n}} A[s(\vec{n},n_t)]\cdot[\rho_\uparrow^{a^\dagger a}(\vec{n}) + \rho_\downarrow^{a^\dagger a}(\vec{n})]\Big\} : . \tag{1.55}$$

By taking the limit $\alpha_t \to 0$ we will obtain the lattice Hamiltonian formalism. In the grand canonical ensemble at chemical potential μ the partition function is

$$\mathcal{Z}(\mu) = \prod_{\vec{n},n_t} \Big[\int ds(\vec{n},n_t) \Big] \operatorname{Tr}\{M(s,L_t-1,\mu)\cdots M(s,0,\mu)\}, \tag{1.56}$$

where

$$M(s,n_t,\mu) = M(s,n_t)\exp\Big\{\mu\alpha_t \sum_{\vec{n}} \rho^{a^\dagger a}(\vec{n})\Big\}. \tag{1.57}$$

To find the ground state energy, let $\left|\Psi_{N,N}^{0,\text{free}}\right\rangle$ be the normalized Slater-determinant representing the ground-state wave function on the lattice for a noninteracting system of N up spins and N down spins. After constructing the Euclidean time projection amplitude we will have

$$\mathcal{Z}_{N,N}(t) = \prod_{\vec{n},n_t} \left[\int ds(\vec{n},n_t) \right] \left\langle \Psi_{N,N}^{0,\text{free}} \middle| M(s,L_t-1) \ \cdots \ M(s,0) \middle| \Psi_{N,N}^{0,\text{free}} \right\rangle, \tag{1.58}$$

where $t = L_t \alpha_t$. We have only single-particle operators interacting with the background auxiliary field and no direct interactions between particles. This is a result of normal ordering. We find

$$\left\langle \Psi_{N,N}^{0,\text{free}} \middle| M(s,L_t-1) \ \cdots \ M(s,0) \middle| \Psi_{N,N}^{0,\text{free}} \right\rangle = \left[\det M(s,t) \right]^2, \tag{1.59}$$

where

$$\left[M(s,t) \right]_{k',k} = \left\langle \vec{p}_{k'} \middle| M(s,L_t-1) \ \cdots \ M(s,0) \middle| \vec{p}_k \right\rangle, \tag{1.60}$$

for matrix indices $k, k' = 1, \cdots, N$. $\left|\vec{p}_{k'}\right\rangle$ and $\left|\vec{p}_k\right\rangle$ are single-particle momentum states comprising the Slater-determinant initial/final state. The single-particle interactions in $M(s,t)$ are the same for both up and down spins, and this is why the determinant in Eq. (1.59) is squared. For the interacting lattice system, we label the energy eigenstates $\left|\Psi_{N,N}^{k}\right\rangle$ with energies $E_{N,N}^{k}$ in order of increasing energy,

$$E_{N,N}^{0} \leq E_{N,N}^{1} \leq \cdots \leq E_{N,N}^{k}. \tag{1.61}$$

In the transfer matrix formalism these energies are defined in terms of the logarithm of the transfer matrix eigenvalue,

$$M \left|\Psi_{N,N}^{k}\right\rangle = e^{-E_{N,N}^{k} \alpha_t} \left|\Psi_{N,N}^{k}\right\rangle. \tag{1.62}$$

We define $c_{N,N}^{k}$ as the inner product with the initial free fermion ground state,

$$c_{N,N}^{k} = \left\langle \Psi_{N,N}^{k} \middle| \Psi_{N,N}^{0,\text{free}} \right\rangle. \tag{1.63}$$

Assume that $c_{N,N}^{k}$, the overlap between free fermion ground state and the interacting ground state, is nonzero. Now we define a transient energy expectation value that depends on the Euclidean time t,

$$E_{N,N} = \frac{1}{\alpha_t} \ln \frac{\mathcal{Z}_{N,N}(t-\alpha_t)}{\mathcal{Z}_{N,N}(t)}. \tag{1.64}$$

After spectral decomposition of $\mathcal{Z}_{N,N}(t)$ we have

$$\mathcal{Z}_{N,N}(t) = \sum_{k} \left| c_{N,N}^{k} \right|^2 e^{-E_{N,N}^{k} t}, \tag{1.65}$$

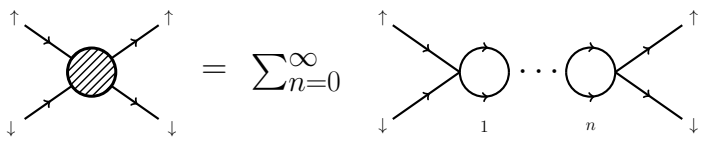

Figure 1.5: Sum of bubble diagrams contributing to two-particle scattering.

and at large Euclidean time t significant contributions come from only low energy eigenstates. For large t we find

$$E_{N,N}(t) \approx E^0_{N,N} + \sum_{k\neq 0} \frac{\left|c^k_{N,N}\right|^2}{\left|c^0_{N,N}\right|^2} \frac{e^{(E^k_{N,N}-E^0_{N,N})\alpha_t}-1}{\alpha_t} e^{(E^k_{N,N}-E^0_{N,N})t}. \tag{1.66}$$

For low energy excitations $E^k_{N,N} - E^0_{N,N}$ is much smaller than the energy cutoff scale α_t^{-1} imposed by the temporal lattice spacing. Therefore

$$E_{N,N}(t) \approx E^0_{N,N} + \sum_{k\neq 0} \frac{\left|c^k_{N,N}\right|^2}{\left|c^0_{N,N}\right|^2} \left(E^k_{N,N} - E^0_{N,N}\right) e^{(E^k_{N,N}-E^0_{N,N})t}. \tag{1.67}$$

The ground state energy $E^0_{N,N}$ is given by the limit

$$E^0_{N,N} = \lim_{t\to\infty} E_{N,N}(t). \tag{1.68}$$

1.5.6 Lüscher finite volume formula

In the previous section we have talked about effective theories regularized by lattice regularization in finite volume (periodic cube). From those methods we can find the energy levels of the system. But these energy levels are measured in finite volume and real physics happens in infinite volume. Now the question is how to connect the measurements in finite volume to the physics. This was done brilliantly by Lüscher [32, 33]. Almost three decades ago Lüscher studied the box size dependence of the energy spectrum in finite volume. He derived a relation connecting the energy levels of an interacting 2-body system in a periodic cube to the infinite volume scattering matrix. Over the years different modifications and generalization to Lüscher's formula have been proposed [34–38]. In the following we will summarize Lüscher's method. We consider two distinguishable particles in a periodic box of length L. The two-particle energy levels in the center-of-mass frame are related to the S-wave phase shift [39],

$$p\cot\delta_0(p) = \frac{1}{\pi L} S(\eta), \qquad \eta = \left(\frac{Lp}{2\pi}\right)^2, \tag{1.69}$$

where $S(\eta)$ is the three-dimensional zeta function with the momentum cutoff Λ,

$$S(\eta) = \lim_{\Lambda\to\infty}\left[\sum_{\vec{n}} \frac{\theta(\Lambda^2 - \vec{n}^2)}{\vec{n}^2 - \eta} - 4\pi\Lambda\right]. \tag{1.70}$$

For $|\eta| < 1$ we can expand $S(\eta)$ in powers of η,

$$\begin{aligned} S(\eta) &= -\frac{1}{\eta} + \lim_{\Lambda\to\infty}\left[\sum_{\vec{n}\neq 0} \frac{\theta(\Lambda^2 - \vec{n}^2)}{\vec{n}^2 - \eta} - 4\pi\Lambda\right], \\ &= -\frac{1}{\eta} + S_0 + S_1\eta + S_2\eta^2 + S_3\eta^3 + \cdots, \end{aligned} \tag{1.71}$$

where

$$S_0 = \lim_{\Lambda\to\infty}\left[\sum_{\vec{n}\neq 0} \frac{\theta(\Lambda^2 - \vec{n}^2)}{\vec{n}^2} - 4\pi\Lambda\right], \qquad S_i = \sum_{\vec{n}\neq 0} \frac{1}{\left(\vec{n}^2\right)^{i+1}}. \tag{1.72}$$

The first few coefficients are

$$\begin{aligned} &S_0 = -8.913631, \quad S_1 = 16.532288, \quad S_2 = 8.401924, \quad S_3 = 6.945808, \\ &S_4 = 6.426119, \quad S_5 = 6.202149, \quad S_6 = 6.098184, \quad S_7 = 6.048263. \end{aligned} \tag{1.73}$$

Lüscher's formula does not include the contribution from higher partial waves but at asymptotically small momenta we can neglect such corrections. The S-wave effective range expansion gives another expression for the left-hand side of Eq. (1.69),

$$p\cot\delta_0(p) \approx -\frac{1}{a_s} + \frac{1}{2}r_0 p^2 + \cdots. \tag{1.74}$$

In terms of η, the energy of the two-particle scattering state is

$$E_{\text{pole}} = \frac{p^2}{m} = \frac{\eta}{m}\left(\frac{2\pi}{L}\right)^2. \tag{1.75}$$

For the case of zero-range interactions, the location of the two-particle scattering pole is calculated by summing the bubble diagrams shown in figure 1.5.

1.6 Ultracold quantum gases

Ultracold atomic gases have been proven to be excellent model systems for studying quantum mechanical phenomena. A system behaves quantum mechanically when the *de Broglie wavelength* of the particles $\lambda = 2\pi\hbar/p$, where p is the momentum of the particles, is of comparable size to the typical spacing between particles. So at sufficiently low energies, the

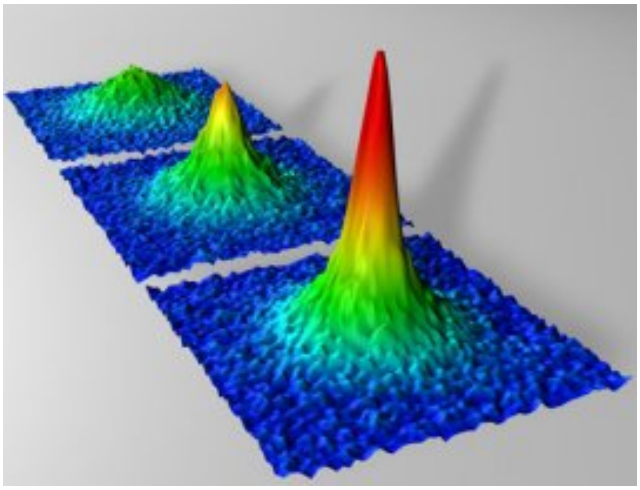

Figure 1.6: Fermionic condensates, shown in surface plots of time-of-flight absorption images. These condensates of generalized Cooper pairs are created at different interaction strengths in the strongly interacting BCS-BEC crossover regime. Picture from [21].

matter wavelength of the particles is the governing length scale of the quantum behavior. For a gas of atoms, with relatively heavy particles and low density, exploring quantum behavior requires cooling the atom gas to extraordinarily low temperatures near absolute zero. This can be achieved with cooling methods like *laser cooling*, *evaporative cooling*, *Doppler cooling*. Only at very low temperatures does it become important that the atoms making up our gas are either bosons or fermions, which are the two classes of quantum particles found in nature. Bosons are particles with integer spin and can occupy identical quantum states. If they are trapped at low enough temperatures, they macroscopically occupy the lowest possible energy state and form a Bose-Einstein condensate (BEC). This condensation elevates quantum behavior to a macroscopic scale and results in fascinating phenomena such as coherent matter waves and superfluidity. On the other hand, fermions have half-integer spin. Fermions must obey the Pauli exclusion principle, which means two indistinguishable fermions are not allowed to occupy the same quantum state. In the limit of absolute zero temperature fermions fill the lowest states with one particle per state in an arrangement known as the Fermi sea.

In many areas of physics such as condensed matter physics, nuclear physics, elementary particle physics, astrophysics, and atomic physics one can see the phenomenon of Bose-Einstein condensation. For example in condensed matter physics we have *Cooper pairs* of electrons in superconductors, ^{4}He atoms in in superfluid liquid He and excitons or

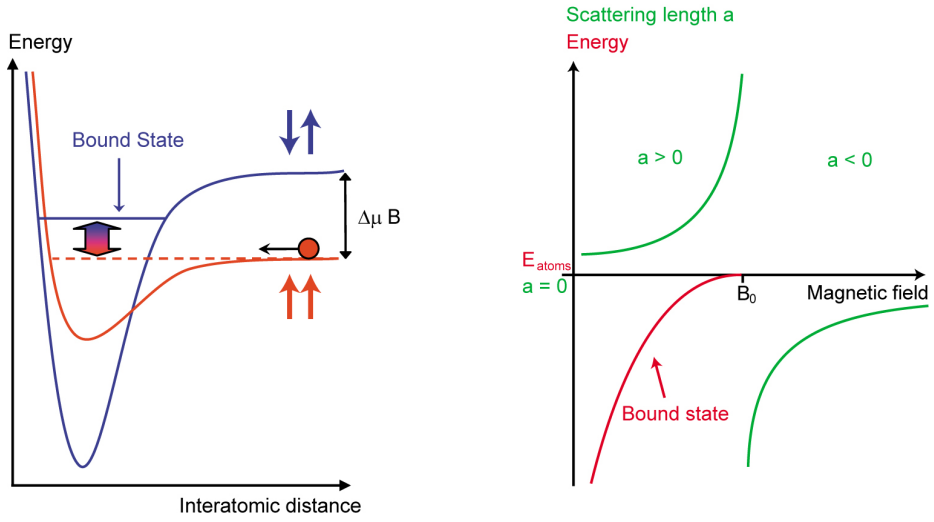

Figure 1.7: Feshbach Resonances and the BEC-BCS crossover. Picture from Lithium-Lab (BEC I).

biexcitons in semiconductors. In nuclear physics and astrophysics we can see neutron pairs or proton pairs in nuclei and also in neutron stars, mesons in neutron star matter, ^{3}He atom pairs in superfluid ^{3}He. As an example in the atomic physics field we have alkali atoms in ultracold atom gases.

These are bosons which condense to a BEC, not fermions. But in many cases an even number of fermions build a composite particle with bosonic quantum number, which can form a Bose-Einstein condensate (See figure 1.6). The fermionic nature of the constituent particles and bosonic nature of the composite particle both play essential roles in condensation phenomena [21, 44, 45]. For instance by studying a system of ^{87}Rb or ^{7}Li (bosonic systems) the underlying fermionic degrees of freedom are irrelevant since the energy which we need to break the atom into two fermions is 10 orders of magnitude larger than the condensation energy. But in a fermionic gas like ^{40}K or ^{6}Li the physicist can explore the connection between fermionic superfluidity (BCS regime) and Bose-Einstein condensation (BEC regime). These can happen through controlling the interaction using a *Feshbach resonance* [24, 25].

A Feshbach resonance occurs when the energy associated to the 2-body scattering (open channel) becomes close to the bound state energy of the pair in a different spin state (close channel). With other words this resonance happens if two slow atoms which collide, may make a transition to a quasi-bound state. As we know in 2-body systems at low energies the only relevant length scale is the scattering length. Using external magnetic fields the

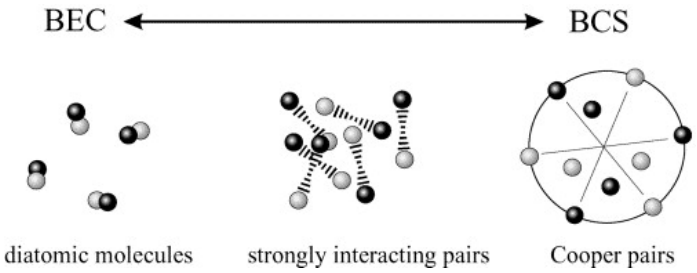

Figure 1.8: (a) In BEC side composite bosons are tightly bound pairs. (c) BCS pairs are correlations of particles on the opposite side of the Fermi momentum sphere. (b) two seemingly distinct regimes of BEC of molecules and BCS superfluidity of Cooper pairs are continuously connected through a BCS-BEC crossover. Picture from [46].

scattering length can be tuned. Since there is a difference between the magnetic moments of the pairs of atoms in the open and closed channel, one can use external magnetic fields to make a transition between these two channels. This transition takes place at some value (B_0) of the magnetic field. We should mention here that if there is no coupling, the existence of the bound state in the closed channel does not affect the scattering in the open channel. The scattering length can be parametrized as a function of the magnetic field B,

$$a(B) = a_{bg}\Big(1 - \frac{\Delta}{B - B_0}\Big), \tag{1.76}$$

where Δ is the width of the resonance and a_{bg} is the background scattering length away from the resonance. By tuning the external magnetic field, the 2-body S-wave scattering length can be varied from noninteracting to strongly interacting. This is shown in figure 1.7. The condensation of Fermi gases is especially interesting. In the strong coupling regime (BEC) the size of the composite particle is smaller than the average interparticle spacing. But in the weak coupling regime (BCS) there is a weak attractive interaction that leads to the formation of Cooper pairs which simultaneously Bose condense. The size of the Cooper pairs is one order of magnitude larger than the average spacing between fermions. At first moment one could think there is no connection between these two cases but actually these two pictures are limiting cases of a more general picture [40], the so called *BCS-BEC crossover* picture. In this picture the condensation behavior in Fermi systems depending on the coupling strength between fermions involves smoothly the well-understood limiting cases. The difference in the size of both sides is shown schematically in picture 1.8.

The last two decades were marked by remarkable experimental achievements in the

physics of cold Fermi gases. Several groups succeeded in cooling trapped fermionic atoms to well below the temperature of quantum degeneracy [18–23]. Fermi systems with essentially any interaction strength can be realized experimentally with ultracold atomic gases. In most experiments, large samples of Alkali atoms (^{6}Li and ^{40}K) are trapped optically in two different hyperfine states. Using the Feshbach resonance, the inter-species S-wave scattering length can be tuned.

Chapter 2

Low-Energy Scattering

At sufficiently low energies, the *de Broglie wavelength* $\lambda = 2\pi\hbar/p$, where p is the momentum of the particles, is the governing length scale of the quantum behavior. If the particles interact through a short-range potential with range r_0 and their relative momentum p satisfies $p \ll \hbar/r_0$, then their de Broglie wavelength prevent them from resolving the structure of the potential. The most important parameter of low-energy interacting particles is the 2-body S-wave *scattering length.* It can be defined in terms of a partial wave expansion for the scattering amplitude. The *natural low-energy length scale* ℓ sets the natural scale for the coefficients in the low-energy expansion of the scattering amplitude. If the magnitude $|a|$ of the scattering length is comparable to ℓ, we say that a has a *natural size.* If $|a| \gg \ell$, we call the scattering length *unnaturally large,* or just *large* to be concise. In the following we will explain some aspects of of low energy physics.

2.1 Unitarity, zero-range limit and universality

The idea of *universality* has its origin in low-energy nuclear physics and has many application in nuclear and particle physics. In modern physics universality refers to situations in which the properties of the system are independent of the dynamical details of the system. In such situations the systems are very different at short distances but they have identical long-distance behavior [41]. In the generic case one can see the universality as a perturbative weak-coupling phenomenon. The role of the coupling constant is played by the scattering length a. There are exceptional cases in which the scattering length can be much larger than the range of interaction, $|a| \gg \ell$. In such cases the concept of universality is still applicable,

but it is a much richer phenomenon. Universal observables are insensitive to the details of short-range interaction. In the 2-body sector, the consequences of universality are simple but nontrivial. For instance, in the case of identical bosons with positive scattering length, there is a 2-body bound state near the scattering threshold with the binding energy

$$E_D = \frac{\hbar^2}{ma^2}. \tag{2.1}$$

The corrections to this formula are small. They are suppressed by powers of r_0/a. We should notice here the dependence of the binding energy on the scattering length a. This dependence is nonperturbative and reflects the fact that universality in the case of a large scattering length is a nonperturbative strong-coupling phenomenon. A classical example of such a system are ^4He atoms.

In the 3-body sector the first evidence for universality was the discovery of the *Efimov effect*. This effect is predicted by the Russian physicist V. N. Efimov in the early 70ties [42]. The Efimov effect can occur in 3-body systems if at least two of three pairs have a large S-wave scattering length. If the Efimov effect occurs, there are infinitely many, arbitrary-shallow 3-body bound states. These bound states have binding energies which have an accumulation point at the 2-body scattering threshold. As the threshold is approached, the ratio of the binding energies of successive states approaches a universal constant. The corrections to the universal behavior are suppressed by powers of $\ell/|a|$. There are two limits in which the size of these corrections decreases to zero, the *resonant limit* ($a \to \pm\infty$ with fixed ℓ) and the *scaling limit* ($\ell \to 0$ with fixed a).

The *resonant limit* describes interacting systems where the range of the interaction is zero and the scattering length is infinite. This limit is also called the *unitarity limit,* because the S-wave cross section saturates the limit imposed by unitarity, $\sigma^{(L=0)} \leq 8\pi/k^2$, for low momenta k. The resonant limit can be approached usually by tuning a single parameter. This parameter could be the depth of interaction or an overall rescaling of the potential. In figure 2.1 (b), the parameter must be tuned to a critical value for which there is a 2-body bound state exactly at the 2-body threshold (Feshbach resonance). In the case of Feshbach resonance, the resonant limit can be approached by tuning the magnetic field. Since $a \to \pm\infty$ in the resonant limit, the only length scale at low energies in the 2-body system is the natural low-energy length scale ℓ. In the 3-body system the Efimov effect reveals that there is another length scale. Physics near the *unitarity limit* has been experimentally observed in cold degenerate gases of ^{6}Li and ^{40}K atoms. The *scaling limit,* also sometimes is called

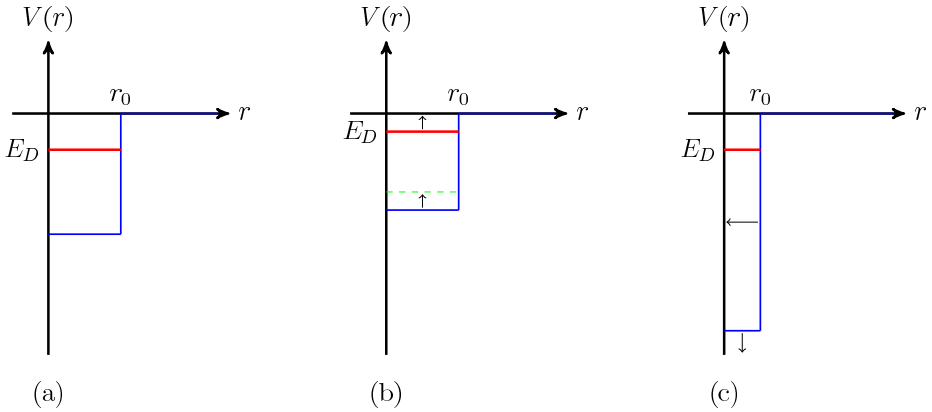

Figure 2.1: (a) A square-well potential with a single shallow bound state, (b) a potential with the same range r_0 that is approaching the resonant limit $E_D \to 0$, and (c) a potential with the same binding energy E_D as in (a) that is approaching the scaling limit $r_0 \to 0$. Inspired by [41]

zero-range limit, is another powerful concept. It can be defined by specifying the phase shifts for 2-body scattering. In this limit, the S-wave phase shift $\delta_0(k)$ has the simple form

$$k \cot \delta_0(k) = -1/a, \tag{2.2}$$

and the phase shifts for all higher partial waves vanish. To approach the scaling limit one needs to tune multiple parameters in the interparticle potential. For example, as illustrated in figure 2.1 (c), it can be reached by simultaneously tuning the range of the potential to zero and its depth to ∞ in a such way that the binding energy of the shallowest 2-body bound state remains fixed. In the scaling limit the scattering length a sets the scale for low-energy observables in the 2-body sector. In the 3-body sector, observables can also have logarithmic dependence on a second scale because of the Efimov effect.

2.2 Fermi gas at unitarity

In this part of the thesis we consider the unitarity limit of two-component fermions. Throughout our discussion we refer to the two degenerate components as up and down spins, though the correspondence with actual spin is not necessary. In the unitarity limit details about the microscopic interaction are lost, and the system shows universal properties. At sufficiently low temperatures the spin-unpolarized system is an S-wave superfluid with properties in between a BCS fermionic superfluid at weak coupling and a BEC of dimers

at strong coupling. As we mentioned before the ground state in the BCS limit has a large size since the Cooper pairs are very shallow bound and the ground state in the BEC limit is tightly bound. At the unitarity limit the ground state has strongly interacting pairs. The size of these pairs are comparable to the Fermi momentum. This is shown schematically in figure 2.2.

In nuclear physics the phenomenology of the unitarity limit approximately describes cold dilute neutron matter which is believed to be relevant physics of the inner crust of the neutron stars [43]. The scattering length for elastic neutron-neutron collisions is $a_{nn} \simeq -18$ fm. For densities $\rho > 10^{-4}\rho_N$, with $\rho_N \simeq 0.16$ fm^{-3} the saturation density of nuclear matter, the dimensionless parameter $k_F|a_{nn}|$ is much bigger than one. Here k_F represents the Fermi momentum. On the other hand the effective range of elastic neutron-neutron collisions is $r_{nn} \simeq 2.8$ fm and so for densities like $\rho < 0.1\rho_N$, the dimensionless parameter $k_F|r_{nn}|$ is very small. For densities like $10^{-4}\rho_N < \rho < 0.1\rho_N$ the neutron matter is very close to the limit in which $k_F|a_{nn}| \to \infty$ and $k_F|r_{nn}| \to 0$ and so the unitarity limit is approximately realized. These conditions cannot be produced experimentally, neutrons at around this density can be found in the inner crust of neutron stars. At the unitarity limit the scattering length diverges while the range of interaction vanishes. From the effective range expansion Eq. (1.8) we know that for the S-wave, $p \cot \delta_0 \approx 0$. As we know the S-wave scattering amplitude is given by

$$\mathcal{A}_0 = \frac{1}{p \cot \delta_0 - ip} \tag{2.3}$$

and so at the unitarity limit the S-wave amplitude, $\mathcal{A}_0 \to i/p$, dose not depend on details of the interaction.

Experimental probes of the unitarity limit are now well established using trapped ultracold Fermi gases of alkali atoms. The characteristic length scale for the interatomic potential is the van der Waals length ℓ_{vdW}. In the dilute limit the spacing between atoms can be made much larger than ℓ_{vdW} and the interatomic potential is well approximated by a zero-range interaction. The S-wave scattering length can be tuned using a magnetic Feshbach resonance. This technique involves setting the energy level for a molecular bound state in a "closed" hyperfine channel to cross the scattering threshold for the "open" channel. The total magnetic moments for the two channels are different, and so the crossing can be produced using an applied magnetic field.

Back to the theory, it was in the late nineties that George Bertsch asked himself what

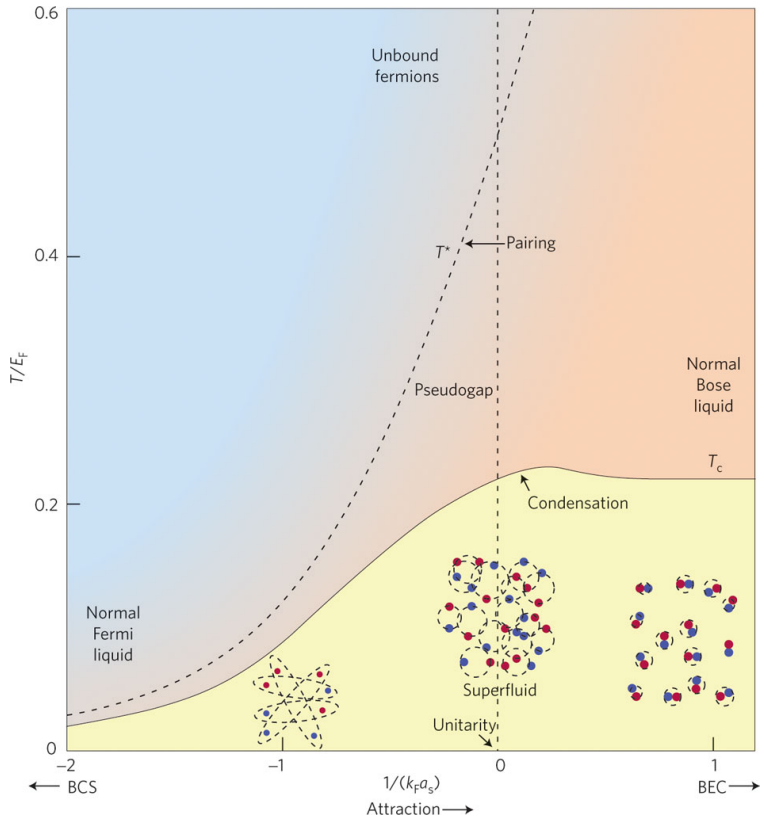

Figure 2.2: BCS-BEC crossover. Picture from [47]

are the ground state properties of the many-body system made of fermions at the unitarity limit. The ground state for two-component fermions in the unitarity limit has no physical length scales other than the average distance between particles. The scaling properties in the unitarity limit are the same as that of a non-interacting Fermi gas and therefore the ground state properties are proportional with a dimensionless universal parameter as proportionality constant. At the unitarity limit this universal constant gives the thermodynamic quantities and it is called *Bertsch parameter*.

For $N_\uparrow$ up spins and $N_\downarrow$ down spins in a given volume we write the energy of the unitarity-limit ground state as $E^0_{N_\uparrow,N_\downarrow}$. For the same volume we call the energy of the free non-interacting ground state $E^{0,\text{free}}_{N_\uparrow,N_\downarrow}$. In the following we write the dimensionless ratio of the two energies as $\xi_{N_\uparrow,N_\downarrow}$,

$$\xi_{N_\uparrow,N_\downarrow} = E^0_{N_\uparrow,N_\downarrow}/E^{0,\text{free}}_{N_\uparrow,N_\downarrow}. \tag{2.4}$$

The parameter ξ is defined as the thermodynamic limit for the spin-unpolarized system,

$$\xi = \lim_{N\to\infty} \xi_{N,N}. \tag{2.5}$$

There are several experimental measurement for the Bertsch parameter, ξ using different methods like using the expansion rate of ^{6}Li and ^{40}K released from a harmonic trap or sound propagation [50–52, 54–56, 58]. There are also numerous analytical and numerical calculations of ξ in the literature which can be found in [48]. We summarized most of these measurements and calculations in tables 2.1, 2.2 and 2.3. Our goal is to find a benchmark for ξ by calculating it for the smallest possible system namely the 4-body system. We start with the free nonrelativistic lattice Hamiltonian and the spin-density operators which we defined in Eq. (1.34) and Eq. (1.46). We consider two different lattice Hamiltonians, each of which yield the unitarity limit in the low-energy limit. The first Hamiltonian H_1 has a single-site contact interaction,

$$H_1 = H_{\text{free}} + C_1 \sum_{\vec{n}} \rho_\uparrow(\vec{n})\rho_\downarrow(\vec{n}). \tag{2.6}$$

The second Hamiltonian H_2 has a contact interaction as well as nearest-neighbor interaction terms,

$$\begin{aligned} H_2 = H_{\text{free}} &+ C_2 \sum_{\vec{n}} \rho_\uparrow(\vec{n})\rho_\downarrow(\vec{n}) \\ &+ C_2' \sum_{\mu=1,2,3} \sum_{\vec{n}} [\rho_\uparrow(\vec{n})\rho_\downarrow(\vec{n}+\hat{\mu}) + \rho_\uparrow(\vec{n}+\hat{\mu})\rho_\downarrow(\vec{n})]. \end{aligned} \tag{2.7}$$

We use Lüscher's formula Eq. (1.69) to determine the coefficients of interaction in Eq. (2.6) and Eq. (2.7). The coefficient of C_1 is tuned to set the S-wave scattering length a_s to infinity. The coefficients C_2 and C_2' are tuned so that a_s goes to infinity while the S-wave effective range parameter r_0 vanishes. Setting a_s to infinity requires $p\cot\delta_0(p)$ to vanish at threshold. Setting both a_s to infinity and r_0 to zero requires that $p\cot\delta_0(p)$ is $O(p^4)$ near threshold. The plots for $p\cot\delta_0(p)$ versus p^2 are shown in figure 2.3. The values we find for the interaction coefficients are

$$mC_1 = 3.9570, \tag{2.8}$$

$$mC_2 = 3.7235, \qquad mC'_2 = 0.3008. \tag{2.9}$$

We have computed the ground-state energy for two spin-up and two spin-down particles in

Method	Collaboration	ξ
measurement of energy of trapped Fermi gas	O'Hara *et al.* [49]	0.6(1)
measurement of the size of the atomic cloud	Bartenstein *et al.* [50]	$0.27^{+0.12}_{-0.09}$
measurement of speed of sound in trapped Fermi gas	Kinast *et al.* [51]	0.430(15)
measurement of the cloud size of the Fermi gas	Thomas *et al.* [52]	0.39(2)
measurement of energy-entropy of trapped unitary Fermi gas	Thomas *et al.* [53]	0.41(2)
measurement of energy of Fermi gas from expansion energies	Bourdel *et al.* [54]	0.360(15)
measurement of potential energy of ultra-cold trapped Fermi gas	Stewart *et al.* [55]	$0.46^{+0.05}_{-0.12}$
measurement of speed of sound in trapped Fermi gas	Joseph *et al.* [56]	0.435(15)
direct measurement the equation of state of the uniform gas	Nascimbene *et al.* [57]	0.51(2)
measurement of the spatial size of the paired Fermi gas	Partridge *et al.* [58]	0.46(5)

Table 2.1: Experimental measurements of ξ.

Method	Collaboration	ξ
calculation based of Galitskii resummation	Heiselberg *et al.* [59]	0.68
calculation based of Pade' approximants	Baker *et al.* [60]	0.68
calculation that includes pairing fluctuations beyond mean field	Perali *et al.* [61]	0.455
NSR approximation of T-matrix (fully-self-consistent scheme)	Drummond *et al.* [62]	0.36
density functional equation	Adhikari *et al.* [63]	0.35
ϵ expansion including the next-to-next-to-leading-order	Nishida *et al.* [64]	0.36(2)
density-functional theory for fermions in the unitary regime	Papenbrock *et al.* [65]	0.42
renormalization group	Krippa *et al.* [66]	0.62
Large-N expansion for unitary superfluid Fermi gases	Veillette *et al.* [67]	0.28
applying effective field theory to finite-density systems	Steele *et al.* [68]	0.54

Table 2.2: Analytical calculation of ξ.

a periodic cube of length L by diagonalizing the scattering matrix using Lanczos algorithm. For both lattice Hamiltonians, H_1 and H_2, we have computed $\xi_{2,2}$ as defined in Eq. (2.4) for values of $L = 4, 5, 6, 7, 8$. The results are shown in figure 2.4. We have fitted the data using polynomials in $1/L$ up to third order and extrapolate to the infinite L limit with an estimated extrapolation error of ± 0.002. We note that this extrapolation should remove all

Method	Collaboration	ξ
fixed-node Green's function Monte Carlo	Carlson *et al.* [69]	0.42(1)
determinant diagrammatic Monte Carlo method	Burovski *et al.* [70]	0.493(14)
auxiliary field quantum Monte Carlo	Bulgac *et al.* [71]	0.37(5)
fixed-node diffusion Monte Carlo method	Astrakharchik *et al.* [72]	0.42(1)
Hybrid Monte Carlo	Lee *et al.* [73]	0.25(3)
Restricted Path Integral Monte Carlo	Akkineni *et al.* [74]	0.42
Monte Carlo calculation	Abe *et al.* [75]	0.292(24)
the heavy-light ansatz	Lee *et al.* [76]	0.31(1)
sign-restricted mean-field lattice calculation	Juillet *et al.* [77]	0.449(9)
fixed-node Green's function Monte Carlo	Chang *et al.* [78]	0.44(1)

Table 2.3: Numerical determination of ξ.

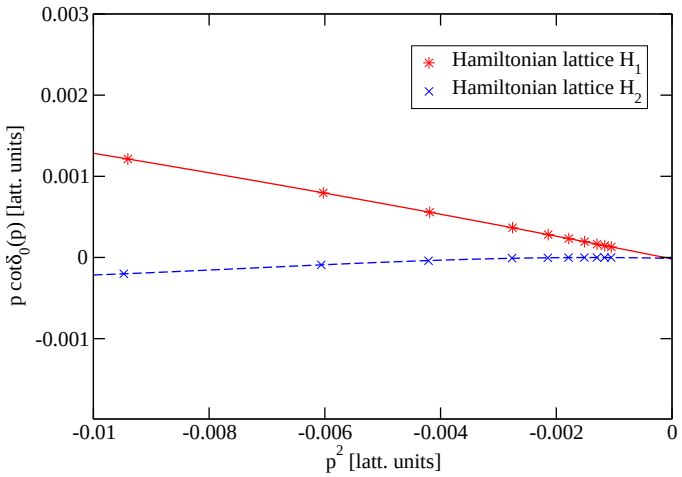

Figure 2.3: Plot of $p \cot \delta_0(p)$ versus p^2 for the lattice Hamiltonians H_1 and H_2.

measurable lattice discretization effects. For H_1 we find

$$\xi_{2,2} = 0.211(2), \tag{2.10}$$

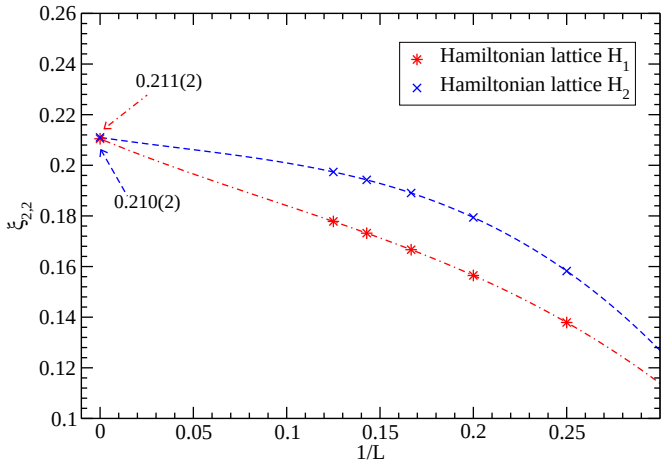

Figure 2.4: Ground-state energy ratio $\xi_{2,2}$ for lattice Hamiltonians H_1 and H_2. We show results for values of $L = 4, 5, 6, 7, 8$ and extrapolate to the infinite volume limit.

and for H_2 we get

$$\xi_{2,2} = 0.210(2). \tag{2.11}$$

The agreement between these two independent calculations is consistent with our estimate of the systematic errors. For the extrapolation to the continuum we use a third-degree polynomial function. This is made possible by the high-precision data obtained for each L using the Lanczos eigenvector iteration. For the H_2 data we note the small slope in $1/L$ near $1/L = 0$. This is expected due to the effective range r_0 being set to zero for H_2. The small amount of linear dependence in $1/L$ that remains is likely due to other lattice artifacts, such as the breaking of Galilean invariance. This numbers are in excellent agreement with the Euclidean lattice and diffusion Monte Carlo calculations. The values calculated for the Bertsch parameter using Euclidean lattice and diffusion Monte Carlo are 0.206(9) and 0.212(2) respectively. Also this benchmark is used to confirm another study [79].

2.3 Bound States moving in a finite volume

In this section we consider finite-volume effects of composite particles in motion. We discuss corrections to the binding energies of bound states in a moving frame. We also show

how the finite-volume scattering method is modified if one or both particles are composite. This modification of Lüscher's formula has an immediate application in nuclear and cold atom physics. As derived by Lüscher the energy shift for a dimer at rest when it is placed in a periodic cube of volume L^3 is

$$\Delta E_{\vec{0}} \approx \sum_{|\vec{n}|=1} \int d^3r \; \phi^*_\infty(\vec{r}) V(\vec{r}) \phi_\infty(\vec{r} + \vec{n}L), \tag{2.12}$$

where $V(\vec{r})$ is the interaction potential and ϕ_∞ is the infinite-volume wavefunction as a function of the relative separation $\vec{r}$. The summation is over integer vectors $\vec{n}$ with magnitude 1. Throughout our discussion, we assume that the energies and momenta are nonrelativistic. For finite-range interactions Eq. (2.12) gives a correction which scales as $e^{-\kappa L}/L$ in the large volume limit, where κ is the binding momentum.

We now consider a dimer moving in the same periodic cube with momentum $2\pi\vec{k}/L$ for integer $\vec{k}$. In the dimer wavefunction we can factorize out the phase dependence due to the center-of-mass motion,

$$\psi_L(\vec{r}_1, \vec{r}_2) = e^{i2\pi\alpha\vec{k}\cdot\vec{r}_1/L} \; e^{i2\pi(1-\alpha)\vec{k}\cdot\vec{r}_2/L} \phi_L(\vec{r}_1 - \vec{r}_2), \tag{2.13}$$

where $\alpha = m_1/(m_1 + m_2)$. Since $\psi_L(\vec{r}_1, \vec{r}_2)$ is periodic in $\vec{r}_1$ and $\vec{r}_2$, ϕ_L gets a nontrivial phase for each winding around the toroidal topology of the periodic cube,

$$\phi_L(\vec{r} + \vec{n}L) = e^{-i2\pi\alpha\vec{k}\cdot\vec{n}/L} \phi_L(\vec{r}), \tag{2.14}$$

for all integer $\vec{n}$. We should mention here that the phase factors have been previously studied in consideration of finite-volume scattering in moving frames [80, 81]. However, the effect of phase factors on bound-state is a qualitatively different effect. The effect of the phase factors is similar to the situation in which we have twisted boundary condition. Each phase twist induces a measurable shift in the binding energy. Now we combine Eq. (2.14) with Eq. (2.12) in order to find the S-wave finite-volume correction in a moving frame. For $\ell = 0$ (S-wave) the asymptotic wavefunction $\phi_\infty(\vec{r})$ is given by

$$\phi_\infty(\vec{r}) = \phi_\infty(|\vec{r}\,|) = \sqrt{\frac{1}{4\pi}} \frac{u_0(r)}{r} = \sqrt{\frac{1}{4\pi}} \frac{\gamma e^{-\kappa r}}{r} \quad \text{for} \quad r > R. \tag{2.15}$$

Here, R represents the range of the potential. Since the potential has a finite range, $R \ll L$, there will be contribution only with $|\vec{r}\,' + \vec{n}\,'L| > R$ in $\Delta E_{\vec{k}}$. So we have for $\Delta E_{\vec{k}}$

$$\Delta E_{\vec{k}} = \frac{\gamma}{\sqrt{4\pi}} \sum_{|\vec{n}|=1} \int d^3\vec{r} \int d^3\vec{r}\,' \; \phi^*_\infty(|\vec{r}\,|) V(\vec{r}, \vec{r}\,') e^{-i\vec{\theta}\cdot\vec{n}} \frac{e^{-\kappa|\vec{r}\,' + \vec{n}L|}}{|\vec{r}\,' + \vec{n}L|} + O\big(e^{-\sqrt{2}\kappa L}\big), \tag{2.16}$$

where $\vec{\theta} = 2\pi\alpha\vec{k}$. Using the equation of motion we can eliminate the potential. So for the energy shift we will obtain

$$\Delta E_{\vec{k}} = \frac{\gamma}{\sqrt{4\pi}} \sum_{|\vec{n}|=1} \int d^3\vec{r} \left[\left(\frac{\nabla^2}{2\mu} - E \right) \phi^*_\infty(|\vec{r}|) \right] \frac{e^{-\kappa|\vec{r}\,'+\vec{n}L|}}{|\vec{r}\,' + \vec{n}L|} e^{-i\vec{\theta}\cdot\vec{n}} + O\big(e^{-\sqrt{2}\kappa L}\big). \tag{2.17}$$

We shift the integration variable and use the partial integration and the fact that $\exp(-\kappa r)/(4\pi r)$ is the Green's function of the operator $\big(\nabla^2 - \kappa^2\big)$. So we get

$$\begin{aligned}
\Delta E_{\vec{k}} &= \frac{\gamma}{\sqrt{4\pi}} \sum_{|\vec{n}|=1} \int d^3\vec{r}\, \phi^*_\infty(|\vec{r} - \vec{n}L|) \frac{1}{2\mu} \big(\nabla^2 - \kappa^2\big) \frac{e^{-\kappa r}}{r} e^{-i\vec{\theta}\cdot\vec{n}} + O\big(e^{-\sqrt{2}\kappa L}\big), \\
&= -\frac{\sqrt{\pi}\gamma}{\mu} \sum_{|\vec{n}|=1} \phi^*_\infty(|\vec{n}L|) e^{-i\vec{\theta}\cdot\vec{n}} + O\big(e^{-\sqrt{2}\kappa L}\big), \\
&= -\frac{\sqrt{\pi}\gamma}{\mu} \phi^*_\infty(L) \sum_{\ell=1}^{3} \left(e^{i\theta_\ell} + e^{-i\theta_\ell} \right) = -\frac{2\sqrt{\pi}\gamma}{\mu} \phi^*_\infty(L) \sum_{\ell=1}^{3} \cos\theta_\ell.
\end{aligned} \tag{2.18}$$

The finite-volume correction in the binding energy of a dimer with momentum $2\pi\vec{k}/L$ in terms of the energy shift in the rest frame is given by

$$\frac{\Delta E_{\vec{k}}}{\Delta E_{\vec{0}}} \approx \frac{1}{3} \sum_{\ell=1}^{3} \cos(2\pi\alpha k_\ell) \equiv \tau(\vec{k}, \alpha). \tag{2.19}$$

The computational advantage of this approach is that finite-volume effects can be directly removed from lattice data without extrapolating to large lattice volumes. This is especially useful for the case with more than two constituents where the analytic form for the finite-volume L-dependence is a *priori* unknown. These corrections have a universal dependence on momentum determined by the number and mass of the constituents. In asymptotically large volumes the corrections are exponentially small and can be neglected. But if the volume is relatively small, this shift can be comparable to that of the scattering process of the dimer. This is shown in figure 2.5.

We now turn our attention to the scattering of composite states in a finite periodic cube. We consider the scattering between states A and B in the center-of-mass frame. Let μ_{AB} be the reduced mass, and let $E_{AB}(p, L)$ be the total energy of the A-B scattering system with radial momentum p in a periodic cube of length L. The states A and B can be point particles or composite bound states. We assume that the constituent particles comprising the states have finite range interactions. The composite structures of A and B, however, will in general produce effective interactions with exponential tails extending to infinity. These

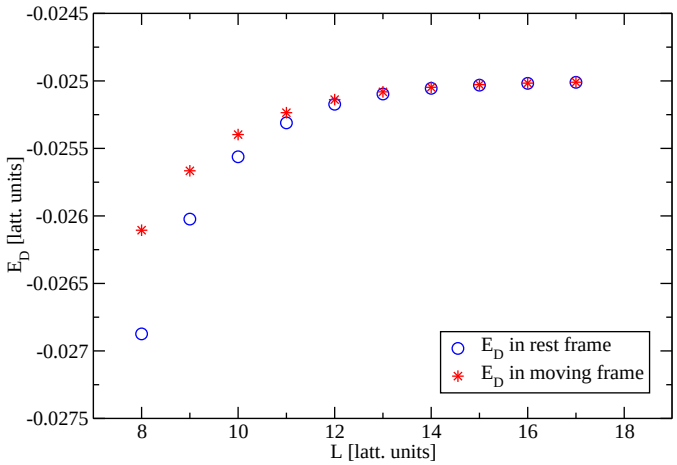

Figure 2.5: Ground-state energy of the dimer with the binding energy of -0.025 in lattice units in the rest and moving frame.

tails generate exponentially small finite-volume corrections to $E_{AB}(p, L)$ associated with the binding energies of A and B separately as well as the scattering of A and B together. We will not be concerned with exponentially small corrections to the scattering of A and B. If the interactions between A and B are very strong, then it is theoretically possible that the finite-volume scattering corrections we neglect are comparable to the binding energy shifts. However, in such cases the part of the energy shift due to scattering which is not exponentially suppressed will be much larger still, and so the loss of accuracy in the scattering analysis will be small.

In order to calculate finite-volume corrections due to the binding energy, it suffices to consider singular solutions of the free Helmholtz equation. Let $\vec{r}$ be the separation between the center of masses of the two states. In the following we assume that p is sufficiently small so that angular momentum mixing with higher-order singular solutions can be neglected. For S-wave scattering between states A and B with radial momentum p, the position-space scattering wavefunction is

$$\left\langle \vec{r} \middle| \Psi_p \right\rangle = c \sum_{\vec{k}} \frac{e^{i(2\pi\vec{k}/L)\cdot\vec{r}}}{(2\pi\vec{k}/L)^2 - p^2} \tag{2.20}$$

with some normalization constant c. Let $E^A_{\vec{k}}(L)$ and $E^B_{-\vec{k}}(L)$ be the finite-volume energies

due to binding for bound states A and B with momenta $2\pi\vec{k}/L$ and $-2\pi\vec{k}/L$, respectively. For point particles without internal structure, these energies are by definition zero for all momenta. The total energy $E_{AB}(p,L)$ is then

$$E_{AB}(p,L) = \frac{\langle\Psi_p|H|\Psi_p\rangle}{\langle\Psi_p|\Psi_p\rangle} = \frac{1}{\mathcal{N}}\sum_{\vec{k}} \frac{\frac{p^2}{2\mu_{AB}} + E^A_{\vec{k}}(L) + E^B_{-\vec{k}}(L)}{(\vec{k}^2-\eta)^2}, \tag{2.21}$$

where $\mathcal{N} = (\vec{k}^2-\eta)^{-2}$ and $\eta = p^2L^2/(2\pi)^2$. The finite-volume correction can be written as

$$E_{AB}(p,L) - E_{AB}(p,\infty) = \tau_A(\eta)\Delta E^A_{\vec{0}}(L) + \tau_B(\eta)\Delta E^B_{\vec{0}}(L), \tag{2.22}$$

where $\Delta E^A_{\vec{0}}(L)$ and $\Delta E^B_{\vec{0}}(L)$ are the finite-volume corrections for states A and B at rest, and we have defined the *topological volume factor* as

$$\tau(\eta) = \frac{1}{\mathcal{N}}\sum_{\vec{k}}\sum_{\ell=1}^{3} \frac{\cos(2\pi\alpha k_\ell)}{3(\vec{k}^2-\eta)^2}. \tag{2.23}$$

The finite-volume correction in Eq. (2.22) has nothing to do with the interaction between states A and B and should therefore be subtracted from the total energy before using Lüscher's scattering relation. This subtraction should reduce systematic errors in lattice calculations. This is demonstrated in the following section.

2.4 Elastic fermion-dimer scattering

The scattering between a fermion and a weakly bound dimer consisting of two fermions is important in nuclear physics (neutron matter) and in the physics of ultracold Fermi gases. This kind of scattering was first explored by Skornyakov and Ter-Martirosian [82] in connection with neutron-deuteron scattering. Since then such systems are investigated by many other groups in the context of nuclear physics or ultracold Fermi gases [83–86, 88, 89]. Because of the Pauli principle 3-body bound states (Effimov states) are not permitted. The solution of such scattering systems give the atom-dimer scattering length which is proportional to the 2-body scattering length a,

$$a_{\rm fd} \simeq 1.18a \quad \text{or} \quad \kappa a_{\rm fd} \simeq 1.18, \tag{2.24}$$

where κ represents binding momentum of the dimer and is given by

$$\kappa = \sqrt{m\,E_D} = \frac{1}{a}. \tag{2.25}$$

There is a very good agreement between the results of all groups for the fermion-dimer scattering length. But for the effective range the situation is totally different. There is only one reported determination of effective range [86]. This calculation found $\kappa r_{\rm fd} \approx 0.08(1)$ fm. The small value of effective range is also favored by neutron-deuteron scattering data but the sign of the effective range still remains an open question. In this part we will consider elastic fermion-dimer scattering and calculate the scattering length and effective range of such system. In the analysis presented here we consider scattering between a fermion and a bound dimer composed of two fermions. In order to test the precision of our lattice calculations, we compare it the result of calculations using the Skorniakov-Ter-Martirosian (STM) integral equation.

We consider two component fermions. We will refer to the two fermion components as spin up and spin down and consider the case when the masses are equal, $m_\uparrow = m_\downarrow$. We assume finite-range attractive interactions and consider the universal shallow binding limit. If R is the range of the interactions and κ is the binding momentum of the dimer, then the shallow binding limit corresponds to $\kappa R \to 0$. We show that finite-volume topological corrections to the dimer binding energy must be considered in order to obtain accurate results. Once these topological corrections are included in the finite-volume analysis, we find that the lattice and continuum calculations are in full agreement.

The free non-relativistic Hamiltonian of two-component fermions with only short-range interaction corresponding to the Hamiltonian and spin density operators on the three dimensional lattice is defined in Eq. (1.34) and Eq. (1.46). We consider two independent lattice Hamiltonian Eq. (2.6) and Eq. (2.7). The free Hamiltonian was given as

$$H_{\rm free} = \frac{3}{m}\sum_{\vec{n},i} a_i^\dagger(\vec{n})a_i(\vec{n}) - \frac{1}{2m}\sum_{\vec{n},i}\sum_{\hat{\mu}=\hat{1},\hat{2},\hat{3}}\Big[a_i^\dagger(\vec{n})a_i(\vec{n}+\hat{\mu}) + a_i^\dagger(\vec{n})a_i(\vec{n}-\hat{\mu})\Big], \qquad (2.26)$$

as well as the lattice density operators

$$\begin{aligned}\rho_\uparrow^{a^\dagger a}(\vec{n}) &= a_\uparrow^\dagger(\vec{n})a_\uparrow(\vec{n}),\\ \rho_\downarrow^{a^\dagger a}(\vec{n}) &= a_\downarrow^\dagger(\vec{n})a_\downarrow(\vec{n}).\end{aligned} \qquad (2.27)$$

The two independent Hamiltonian H_1 and H_2 were

$$H_1 = H_{\text{free}} + C_1 \sum_{\vec{n}} \rho_\uparrow(\vec{n})\rho_\downarrow(\vec{n}), \tag{2.28}$$

$$H_2 = H_{\text{free}} + C_2 \sum_{\vec{n}} \rho_\uparrow(\vec{n})\rho_\downarrow(\vec{n}) + C_2' \sum_{\mu=1,2,3} \sum_{\vec{n}} [\rho_\uparrow(\vec{n})\rho_\downarrow(\vec{n}+\hat{\mu}) + \rho_\uparrow(\vec{n}+\hat{\mu})\rho_\downarrow(\vec{n})]. \tag{2.29}$$

The finite lattice spacing error in these two Hamiltonians is of order a_{latt}^2. The next step is to determine the interaction coefficients, C_1, C_2 and C_2' using Lüscher's formula Eq. (1.69). The interaction coefficient C_1 is tuned to construct 2-body binding states (dimers) comprised of one spin-up and one spin-down fermion of energies -1.5 MeV, -2.0 MeV, -2.5 MeV, -3.0 MeV, -3.5 MeV and -4.0 MeV in a large volume ($L = 80$) using the Lanczos method. In such a large volume the finite volume corrections to the dimer binding energy are negligible. In our calculation we take $m = 939$ MeV and $a_{latt}^{-1} = 100$ MeV. To find the interaction coefficients of lattice Hamiltonian H_2 we proceed as follows. Setting the effective range to zero requires that the following relation should be satisfied near threshold

$$\frac{1}{\pi L} S(\eta) = p \cot \delta_0(p) \simeq -\frac{1}{a} + O(p^4). \tag{2.30}$$

The interaction coefficients C_2 and C_2' are tuned in order to give the binding energies listed above for the ground state in a large volume ($L = 80$) and to fulfill Eq. (2.30) for the first excited state. The plot for $p \cot \delta_0(p)$ versus p_2 for the first excited state is shown in figure 2.6. The different values of p are generated by calculating for different box sizes. We note that $p \cot \delta_0(p)$ has zero slope near threshold since we set the effective range to zero. Both Hamiltonians reproduce the same continuum limit of fermions with attractive zero-range interactions. The corresponding values for the interaction coefficients are summarized in table 2.4. We use the interaction coefficients in the table 2.4 and diagonalize both Hamiltonians Eq. (2.28) and Eq. (2.29) utilizing the Lanczos method to determine the ground state energy at rest for the six considered dimers in the periodic volumes L^3 ranging from $L = 6$ to $L = 17$. We also use the same interaction coefficients and diagonalization method to find the ground state energy of the fermion-dimer systems. Now we turn our attention to the fermion-dimer scattering in a periodic cube. It is known that there are exponentially small corrections to the scattering energy of the fermion-dimer system at finite volume due to range effects. We can remove this error by extrapolation to the infinite volume.

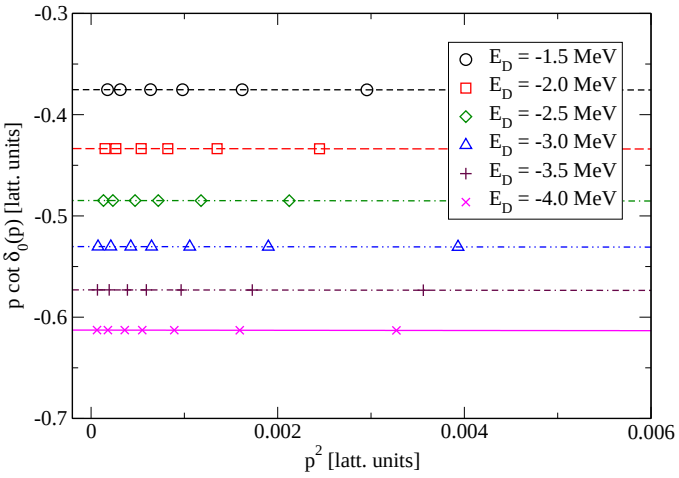

Figure 2.6: Plot of $p \cot \delta_0(p)$ versus p^2 for the lattice Hamiltonian H_2.

E_D	mC_1	mC_2	mC_2'
-0.015	-4.51091	-4.34554	-0.30082
-0.020	-4.61299	-4.45733	-0.34273
-0.025	-4.70675	-4.55883	-0.34658
-0.030	-4.79466	-4.64749	-0.36339
-0.035	-4.87817	-4.73801	-0.36452
-0.040	-4.95823	-4.82374	-0.36696

Table 2.4: The values of interaction coefficients for the six considered dimers. All quantities are given in units of the lattice spacing $a_{\text{latt}} = (100 \text{ MeV})^{-1}$.

However, there is another error which is independent of the fermion-dimer scattering process, namely the finite volume error in the dimer binding energy. We calculate the scattering process in the center-of-mass frame and therefore the dimer has some recoil momentum. In order to find the radial momentum, p, in the fermion-dimer systems, we subtract the binding energies of the dimers in the moving frame from the total scattering energies of the fermion-dimer systems. This difference, $\Delta E(L)$, is the kinetic energy of the fermion-dimer system. We use this to find the radial momentum p.

Now we use the Lüscher's formula with this energy and calculate $p \cot \delta_0(p)$ for six

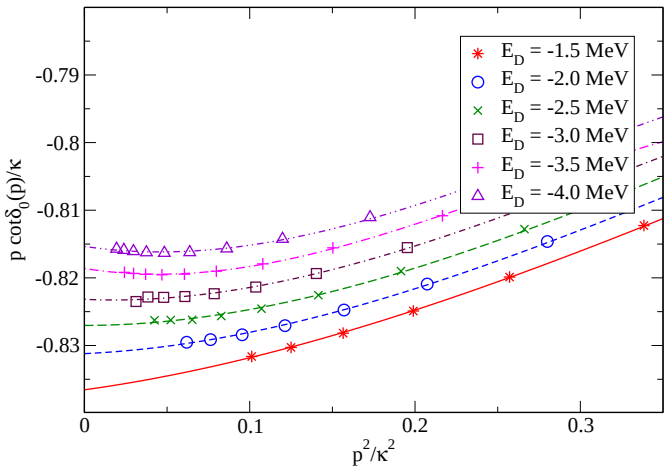

Figure 2.7: Plot of $p \cot \delta_0(p)$ versus p^2 for the lattice Hamiltonian H_1 without topological correction.

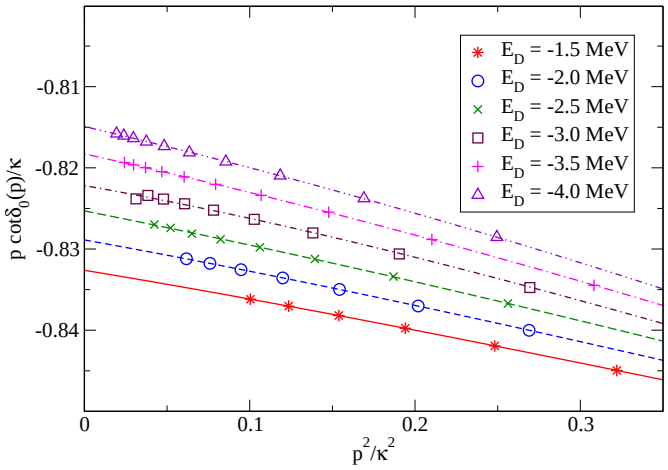

Figure 2.8: Plot of $p \cot \delta_0(p)$ versus p^2 for the lattice Hamiltonian H_1 with topological correction.

different lattice spacings. Here we should mention that calculating $p \cot \delta_0(p)$ for six different dimers is equal to calculating $p \cot \delta_0(p)$ for six different lattice spacing. We also calculate $p \cot \delta_0(p)$ for the case in which we subtracted only the binding energy of the dimer at rest

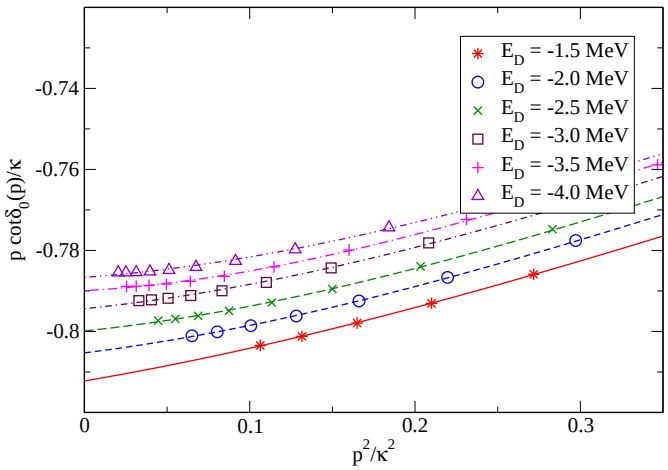

Figure 2.9: Plot of $p \cot \delta_0(p)$ versus p^2 for the lattice Hamiltonian H_2 without topological correction.

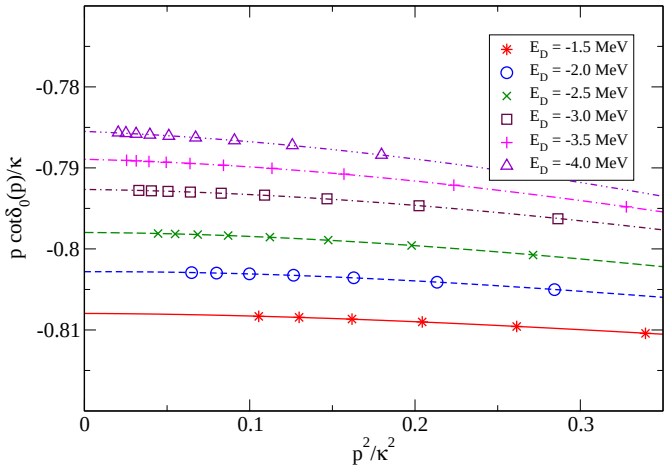

Figure 2.10: Plot of $p \cot \delta_0(p)$ versus p^2 for the lattice Hamiltonian H_2 with topological correction.

frame from the total energy.

To extrapolate to the infinite volume we fit a polynomial of second order to the data points. We write this results as dimensionless combinations multiplied by powers of the

dimer binding momentum κ. By comparing the naive calculation plots in figures 2.7 and 2.9 with the full calculation plots 2.8 and 2.10, we clearly see the effect of the topological phase factor. This correction is quite large for scattering in smaller volumes. The change in slope in plot 2.10 compared to plot 2.8 is expected since we tuned the effective range of interaction to zero for H_2. From these results, we determine the low-energy parameters for fermion-dimer scattering and extrapolate to the continuum limit.

From the lattice calculation of the phase shifts we can extract the effective range parameters. Our results for the scattering length, $a_{\rm fd}$, and the effective range parameter, $r_{\rm fd}$, are shown in figures 2.11 and 2.12. We analyze only the plots in figures 2.8 and 2.10 which contain the full calculations corresponding to H_1 and H_2, respectively. By fitting a polynomial of second order to each set of data we find a scattering length and a effective range in infinite volume for both lattice Hamiltonians. These data points are plotted in figures 2.11 and 2.12. In order to extrapolate to the continuum limit $a_{\rm latt} \to 0$, we use a linear function. The results for the low-energy parameters that we get for these two independent representations of the lattice Hamiltonians are

$$\kappa a_{\rm fd} = 1.162(13), \quad \kappa r_{\rm fd} = -0.041(16) \quad \text{for} \quad H_1, \tag{2.31}$$

$$\kappa a_{\rm fd} = 1.181(7), \quad \kappa r_{\rm fd} = -0.016(16) \quad \text{for} \quad H_2. \tag{2.32}$$

To extrapolate to the continuum limit in the lattice Hamiltonian calculations we used only the data points corresponding to the four smallest lattice spacings. For the other data points, the Compton wavelength of the bound state is comparable to the lattice spacing. We estimate the systematic errors in the continuum extrapolation of the fermion-dimer scattering length and effective range by extrapolation to the continuum limit using only the first two data points and taking the interval between these extrapolation values and the central values obtained using all four data points as the systematic errors. The agreement between these two independent calculations is consistent with our estimate of the systematic errors. As we see from figures 2.11 and 2.12 the inclusion of the topological volume factor $\tau_D(\eta)$ improves the accuracy, especially in the calculation of the effective range parameter. With a very conservative estimation of the systematic error we are able to say that the value of the the fermion-dimer scattering length in units of the dimer binding momentum is in between 1.149 and 1.188. The value of fermion-dimer effective range in units of the dimer binding momentum is between zero and -0.057. Our final result is given by the weighted averages of

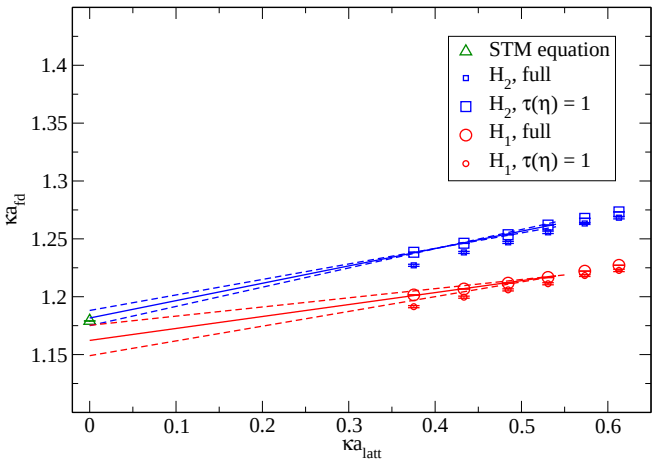

Figure 2.11: Lattice results and continuum extrapolation with error estimates for the fermion-dimer scattering length.

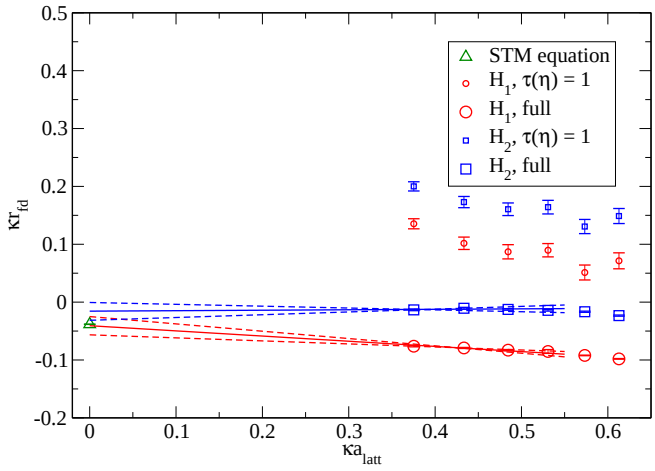

Figure 2.12: Lattice results and continuum extrapolation with error estimates for the fermion-dimer effective range.

the values in Eq. (2.31) and Eq. (2.32):

$$\kappa a_{\rm fd} = 1.174(9), \quad \kappa r_{\rm fd} = -0.029(13). \tag{2.33}$$

In calculating the average, we assumed that the statistical probability distribution of the measured variables are Gaussian and independent of each other. Using standard error propagation, we find the uncertainty in the average values. Our results Eq. (2.33) are in excellent agreement with the continuum calculation using the STM integral equation

$$\kappa a_{\rm fd} = 1.17907(1), \quad \kappa r_{\rm fd} = -0.0383(3). \tag{2.34}$$

The method which we have presented is also used by Rokash *et al.* to study the low-energy neutron-deuteron scattering [87].

Chapter 3

A new look at the polaron problem

One of the fundamental problems in many-body physics is the dynamics of a single impurity in an environment. The impurity couples to the environment and builds up a quasi-particle, a *polaron*. The polaron was first introduced in condensed matter physics and recently has been studied in strongly interacting ultracold Fermi gases [90], a system with many similarities with dilute neutron matter. For ultracold atoms and neutron matter, the polaron can be formed by a spin-down fermion in a sea of $N_\uparrow$ spin-up fermions. Characteristic quantities of a polaron are the interaction energy or binding energy and the effective mass. In three dimensions the polaron state splits into two branches, a low-energy state interacting attractively with the bath of fermions and the repulsive polaron, which is an excited, metastable state [91–93]. In the following we will talk only about attractive polarons.

3.1 Polaron in three dimensions

Until now we talked about balanced Fermi gases but from now on we will consider the extreme case of imbalanced Fermi gases in three dimensions. We study the problem of a single spin-down fermion resonantly interacting with a Fermi gas of spin-up particles. We consider the system of an unitary Fermi gas in three dimensions. The system we are interested in has zero-range interaction and is in the continuum limit. This system has $N_\uparrow$ spin-up particles and one spin-down. One of the characteristic quantities of polaron is the polaron energy which is defined as the energy difference of the system with the polaron added

compared to the free Fermi sea of $N_\uparrow$ spin-up fermions,

$$E_{\rm pol} = E_{N_\uparrow+1} - E_{N_\uparrow}. \tag{3.1}$$

We find the polaron energy in terms of the Fermi energy of the non-interacting system which is given by

$$E_{\rm F} = \frac{k_{\rm F}^2}{2m}, \qquad k_{\rm F} = \left(6\pi^2 \frac{N_\uparrow}{L^3}\right)^{1/3}. \tag{3.2}$$

In the attractive regime, $E_{\rm pol} < 0$ estimates the polaron binding in the Fermi sea. At the limit, where the S-wave scattering length diverges, $a \to \infty$ (unitary limit), the polaron energy is an universal quantity and scales with the Fermi energy, $E_{\rm pol} = \eta E_{\rm F}$. In the attractive regime η is negative and universal.

There are many calculation for the universal polaron energy in three dimensions. A diagrammatic Monte Carlo (DMC) measurement [94] gives $\eta = -0.618$ which is very close to a full-body treatment [95] giving $\eta = -0.6158$ and other quantum Monte Carlo (QMC) calculations [69, 96, 97]. Another study made by Chevy [98] leads to $\eta = -0.6066$. All these theoretical calculations are in very good agreement with each other and all of them are consistent with experimental measured values $\eta = -0.58(5)$ [99] and $\eta = -0.64(7)$ [100]. In [101] the authors generalized the polaron to strongly interacting neutrons when the effective range of the impurity-fermion interaction becomes important.

We begin with the leading order effective Hamiltonian of the system of fermions on the lattice which we represented in the first chapter by Eq. (1.34) and Eq. (1.35) and construct the transfer matrix. The Hamiltonian defined in Eq. (1.35) is also the defining Hamiltonian for the attractive Hubbard model in three dimensions. Roughly speaking the transfer matrix operator is the exponential of the Hamiltonian operator over one Euclidean lattice time step, $e^{-H\alpha_t}$. The transfer matrix operator is given by

$$M =: \exp\big[-H\alpha_t\big] :, \tag{3.3}$$

where $: \cdots :$ denotes normal-ordering. Knowing the transfer matrix lets us to find the correlation function of the system which is given by

$$\mathcal{Z}_{L_t} = \big\langle \Psi_{\rm init} \big| M(L_t - 1) \cdots M(0) \big| \Psi_{\rm init} \big\rangle, \tag{3.4}$$

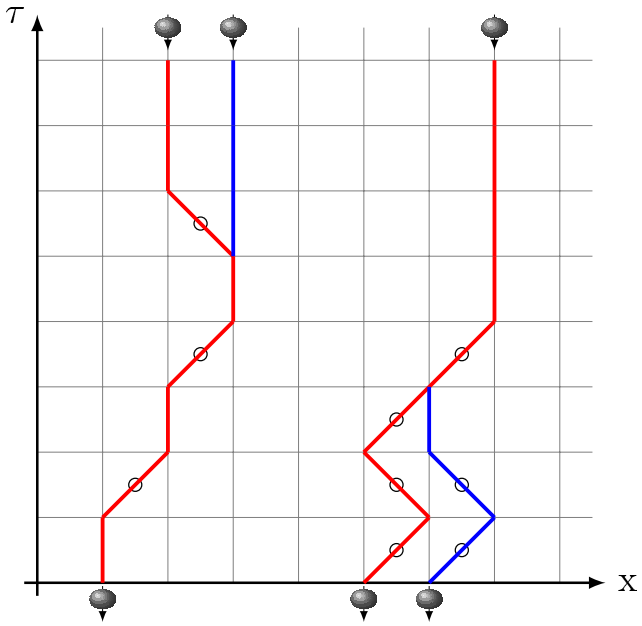

Figure 3.1: Sample worldlines of spin-down fermion on a $1+1$ dimensional lattice. The circles denote a hop during a time step to the neighbor site. On the left hand side worldline the initial point stays the same and on the right hand side the worldline end point remains unchanged.

where $\left|\Psi_{\text{init}}\right\rangle$ is the initial wave function. This initial wave function is the Slater determinant for the non-interacting system. As we mentioned before from the asymptotic behavior of the correlation function we can determine the energy at time t,

$$E(t) = \frac{1}{\alpha_t} \ln \frac{\mathcal{Z}(t-\alpha_t)}{\mathcal{Z}(t)}. \tag{3.5}$$

At large Euclidean time t significant contributions to the energy come from only low energy eigenstates and so as we have shown before the ground state E_0 is given by the limit

$$E_0 = \lim_{t\to\infty} E(t). \tag{3.6}$$

Now we calculate the correlation function by considering explicit spin down fermion worldline. We approximate the value of the correlation function by performing Monte Carlo sampling of the worldlines. In figure 3.1 we show some sample worldlines. The updating procedure for the spin down fermion worldlines are very simple. The time derivative of the worldline at each time step is an hopping index. If the time derivative is not zero, the spin down fermion will hops to the neighbor lattice site and if it is zero, the fermion will stay on the same lattice site. The update simply picks a new value for the hopping index at some given time step.

The new worldline corresponds with regenerating the worldline with the new time derivatives while keeping the initial point or the end-point of the worldline the same.

One general problem by simulating the fermionic systems is so called sign oscillation which is a consequence of the identical particle permutations and there is no general method known for eliminating it in fermionic systems. In our case we have N spin up fermions and one spin down fermion. Suppose we would have N up spins and 0 down spins. Then we would have free gas and the determinant for our given initial/final state would be a positive number. Now consider N up spins and 1 down spin. It seems that the single down spin is not able to change the determinant very much, since it is just 1 down spin compared with N up spins. In the next section we will present some results for three dimensional polaron which are a nice check for the precision of our method.

3.2 Numerical results

We run the simulation for the Fermi systems with different number of down spins in different volumes. This make us able to find the physical value for the polaron energy. First we keep N and L fixed and find the polaron energy of the systems by taking the limit $L_t \to \infty$. We fit the function form $\epsilon + \alpha \exp(-\delta \cdot t)$ to determine the asymptotic value of the ground state energies for each system. We take the continuum limit by extrapolating the energy of each system in $L \to \infty$ limit. We fix the number of particles, N, and set the scattering length equal to infinity, then taking $L \to \infty$ is the same as taking the continuum limit of zero-range interaction. So it is not really an infinite volume limit, but rather a continuum limit. In the three dimensional polaron problem the system is scale-invariant and so we do not have to extrapolate to the limit where the physical volume is infinite. As we mentioned before, the reason we take the limit $L \to \infty$ is so that we can get the continuum limit where the lattice spacing is zero.

In the three dimensional polaron problem the polaron energy in the thermodynamic limit will be some universal constant η times the Fermi energy, E_{F}. We will determine this universal constant η by varying the the number of particles in the box, N, and the length of the box in lattice units, L. By taking $L \to \infty$ we get the continuum limit, and by taking $N \to \infty$ we get the thermodynamic limit. The extrapolation to the continuum limit for four Fermi systems with different number of down spin is shown in figure 3.2. For the extrapolation to the continuum and thermodynamic limit we fit a linear function to the data.

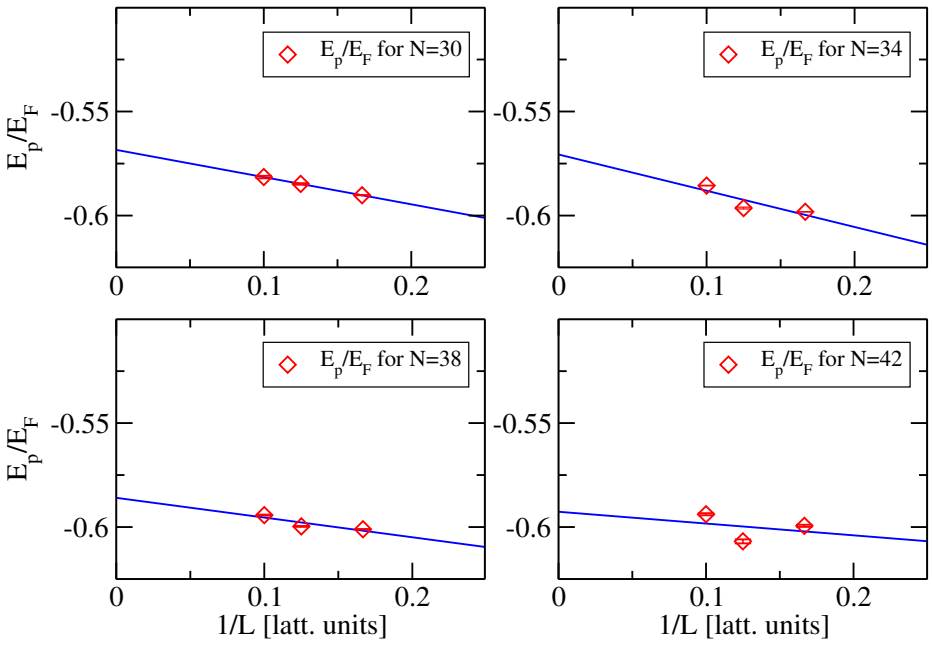

Figure 3.2: The polaron energies as a fraction of Fermi energy for different number of particles.

The value which we obtain for η is

$$\eta = -0.622(11). \tag{3.7}$$

The results of our calculation are shown in figure 3.3. For the comparison we have shown the results of the diagrammatic Monte Carlo (DMC) method done by Prokof'ev and Svistunov [94]. As we can see we have a very good agreement with this value and also the other results in the literature. This shows that the precision of our method is good enough to make further studies particularly the polaron in two spatial dimensions in the future works. In the following we will briefly discuss the two dimensional polaron as an interesting future extension of our method.

3.3 Future extension: polaron in two dimensions

The polaron problem in two dimensions is one of the interesting future applications of our method. Due to the discovery of high-temperature superconductivity of copper oxide compounds [102] fermion's pairing in two dimensions has become one of the interesting themes in physics. Spatial dimensions are very important in polaron physics since the many-body

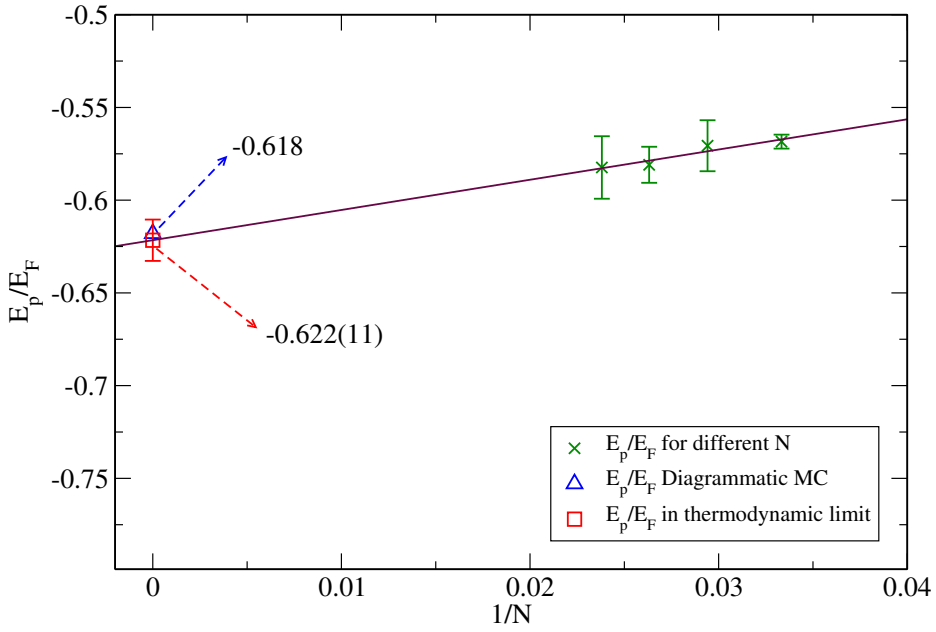

Figure 3.3: The polaron energy as a fraction of Fermi energy.

ground state is affected due to presence of the quantum fluctuations in low dimensions. The properties of Fermi polaron in three dimensions were theoretically predicted [90, 94, 96, 97] and observed experimentally [99, 100]. In one dimension the exact solution to the impurity Hamiltonian can be determined and it does not show any interesting future. The situation in two dimensions is different. There are several theoretical calculations and models which predict different properties for the polaron [103–106].

Experimentally the ultracold atoms are an ideal tool to test various pairing mechanism. In the recent years several experiments probed the Fermi polaron in two dimensions [107–109]. This had led to deeper insight of the Fermi gas in two dimensions. But some questions like the scale invariance (or not) of the two-dimensional Fermi gas [110] remain still open. To this point there is no adequate Monte Carlo simulation for the two-dimensional polaron problem. To clarify the situation and answering the open questions a proper Monte Carlo simulation is missing. Our goal in the future work is to provide a Monte Carlo approach to this problem.

Chapter 4

Summary and outlook

In this work we have presented benchmark calculations for the low-energy scattering regime. Since there is a wide spread in the determined value of the universal constant (Bertsch parameter) in the unitarity limit (0.2 to 0.7) there was a need of a benchmark calculation. We have provided a benchmark result for four unpolarized particles using Hamiltonian lattice eigenvector iteration. We have determined the universal parameter $\xi_{2,2}$ in the unitarity limit for two different Hamiltonians, both of these two Hamiltonians give the unitarity limit in the low-energy limit. We have found

$$\xi_{2,2} = 0.211(2), \qquad \xi_{2,2} = 0.210(2). \tag{4.1}$$

These results have been confirmed by other calculations such as auxiliary-field projection Monte Carlo and fixed-node diffusion Monte Carlo. We have also given a relation for the energy correction to the bound state moving in a periodic cube. We have shown that these corrections contain information about the mass and the number of constituents of the bound states. Since the origin of these corrections is topological we have called them topological volume corrections. Using this relation one can improve the accuracy of the calculations without the need to go to bigger volumes. In figures 2.11 and 2.12 we have demonstrated how the topological volume corrections improved the accuracy of the low-energy parameters in fermion-dimer system. In this thesis we have also demonstrated the lattice calculations for the elastic scattering between a fermion and a bound state in the shallow binding limit. There have been many calculations of the fermion dimer scattering length in this limit. From the very first work done by Skorniakov-Ter-Martirosian [82] to the recent works [83–89] one can find a very nice agreement between all calculated scattering lengths. Neutron-deuteron

scattering in the spin-quartet channel can be described approximately by the fermion-dimer results in the shallow binding limit. Experimental measurements find ${}^4a_{\rm nd}/{}^3a_{\rm np} = 1.17(1)$, where ${}^4a_{\rm nd}$ is the neutron-deuteron scattering length in the spin-quartet channel and ${}^3a_{\rm np}$ denotes the neutron-poroton scattering length in the spin-triplet channel. For the effective-range the situation is completely different. There is only one calculation [86]. In this work we have also determined the effective-range in the shallow binding limit. We have used the finite-volume method of Lüscher and extracted the low-energy parameters from the phase shift calculated for two independent representations of the lattice Hamiltonians. A weighted average of our two calculations gives

$$\kappa a_{\rm fd} = 1.174(9), \quad \kappa r_{\rm fd} = -0.029(13). \tag{4.2}$$

As we mentioned before in order to obtain these values we have used the topological volume corrections. These results have been confirmed by the continuum calculation done by H. -W. Hammer using the STM equation

$$\kappa a_{\rm fd} = 1.17907(1), \quad \kappa r_{\rm fd} = -0.0383(3). \tag{4.3}$$

Both calculations support a small negative effective-range in contrast to the result of [86] which gives a positive small value. In this thesis we have also began the investigation of the Fermi polaron in two dimensions. The quantities which we are interested in are the polaron binding energy and the effective mass of the polaron. We will find these quantities using the Monte Carlo technique to approximate the correlation function. To check the accuracy of our Monte Carlo simulations we have found the binding energy of the attractive Fermi polaron in three dimensions. The value which we have determined for the polaron binding energy in terms of the Fermi energy is

$$E_{\rm p}/E_{\rm F} = -0.622(11). \tag{4.4}$$

This value is in excellent agreement with the calculations or measurements of other groups [69, 94–100] which shows the very good accuracy of the method we use. For the next step we will make a proper Monte Carlo simulation for the two dimensional case since there is no adequate Monte Carlo simulation for the polaron problem in two dimensions. So our goal in future work would be to provide a Monte Carlo approach to this problem.

Bibliography

[1] O. W. Greenberg, "Spin and Unitary-Spin Independence in a Paraquark Model of Baryons and Mesons," Phys. Rev. Lett. **13** (1964) 598.

[2] H. Fritzsch, M. Gell-Mann and H. Leutwyler, "Advantages of the Color Octet Gluon Picture," Phys. Rev. Lett. B **47** (1973) 365.

[3] S. Bethke, "World Summary of α_s (2012)," Nucl. Phys. Proc. Suppl. **234** (2012) 229, [arXiv:hep-ph/1210.0325].

[4] C. P. Burgess, "Introduction to Effective Field Theory," Ann.Rev.Nucl.Part.Sci. **57** (2007) 329-362

[5] A. Pich, "Effective field theory," arXiv:hep-ph/9806303.

[6] B. Kubis, "An Introduction to chiral perturbation theory", arXiv:hep-ph/0703274.

[7] S. Weinberg, "Phenomenological Lagrangians," Physica A **96** (1979) 327.

[8] J. Gasser and H. Leutwyler, "Chiral Perturbation Theory To One Loop," Annals Phys. **158** (1984) 142.

[9] J. Gasser and H. Leutwyler, "Chiral Perturbation Theory: Expansions In The Mass Of The Strange Quark," Nucl. Phys. B **250** (1985) 465.

[10] H. Leutwyler, "On The Foundations Of Chiral Perturbation Theory," Annals Phys. **235** (1994) 165 [arXiv:hep-ph/9311274].

[11] S. Scherer, "Introduction to chiral perturbation theory," Adv. Nucl. Phys. **27** (2003) 277 [arXiv:hep-ph/0210398].

[12] V. Bernard and U.-G. Meißner, "Chiral perturbation theory," Ann. Rev. Nucl. Part. Sci. **57** (2007) 33 [arXiv:hep-ph/0611231].

[13] E. Epelbaum, H. W. Hammer and Ulf -G Meißner, "Modern Theory of Nuclear Forces," Rev. Mod. Phys. **81** (2009) 1773 [arXiv:0811.1338].

[14] S. R. Coleman, J. Wess and B. Zumino, "Structure of phenomenological Lagrangians. 1," Phys. Rev. **177** (1969) 2239.

[15] C. G. Callan, S. R. Coleman, J. Wess and B. Zumino, "Structure of phenomenological Lagrangians. 2," Phys. Rev. **177** (1969) 2247.

[16] P. Lepage, "How to Renormalize the Schrodinger Equation," [arXiv:nucl-th/9706029].

[17] D. B. Kaplan, "Effective Field Theories," [arXiv:nucl-th/9506035].

[18] B. DeMarco and D. S. Jin, "Onset of Fermi Degeneracy in a Trapped Atomic Gas," Science **285**, 1703 (1999).

[19] , Z. Hadzibabic, C. A. Stan, K. Dieckmann, S. Gupta, M. W. Zwierlein, A. Görlitz and W. Ketterle, "Two-Species Mixture of Quantum Degenerate Bose and Fermi Gases," Phys. Rev. Lett. **88** (2002) 160401.

[20] Z. Hadzibabic, C. A. Stan, S. Gupta, C. H. Schunck, M. W. Zwierlein, K. Dieckmann and W. Ketterle, "Fiftyfold Improvement in the Number of Quantum Degenerate Fermionic Atoms," Phys. Rev. Lett. **91** (2003) 160401.

[21] C. A. Regal, M. Greiner and D. S. Jin, "Observation of Resonance Condensation of Fermionic Atom Pairs," Phys. Rev. Lett. **92** (2004) 040403.

[22] F. Schreck, L. Khaykovich, K. L. Corwin, G. Ferrari, T. Bourdel, J. Cubizolles and C. Salomon, "Quasipure Bose-Einstein Condensate Immersed in a Fermi Sea," Phys. Rev. Lett. **87** (2001) 080403.

[23] A. G. Truscott, K. E. Strecker, W. I. McAlexander, G. B. Partridge and R. G. Hulet, "Observation of Fermi Pressure in a Gas of Trapped Atoms," Science **291**, 2570 (2001).

[24] W. C. Stwalley, "Stability of Spin-Aligned Hydrogen at Low Temperatures and High Magnetic Fields: New Field-Dependent Scattering Resonances and Predissociations," Phys. Rev. Lett. **37** (1976) 1628.

[25] S. L. Cornish, N. R. Claussen, J. L. Roberts, E. A. Cornell and C. E. Wieman, "Stable ^{85}Rb Bose-Einstein Condensates with Widely Tunable Interactions," Phys. Rev. Lett. **85** (2000) 1795.

[26] D. Lee, "Lattice simulations for few- and many-body systems," Prog. Part. Nucl. Phys. **63** (2009) 117, [arXiv:nucl-th/0804.3501].

[27] D. Lee, "The Ground state energy at unitarity," Phys. Rev. C **78** (2008) 024001, [arXiv:nucl-th/0803.1280].

[28] B. Borasoy, E. Epelbaum, H. Krebs, D. Lee and U. -G. Meißner, "Lattice Simulations for Light Nuclei: Chiral Effective Field Theory at Leading Order," Eur. Phys. J. A **31** (2007) 105, [arXiv:nucl-th/0611087].

[29] D. Lee and T. Schäfer, "Cold dilute neutron matter on the lattice. II. Results in the unitary limit," Phys. Rev. C **73** (2006) 015202, [arXiv:nucl-th/0509018].

[30] D. Lee and T. Schäfer, "Neutron matter on the lattice with pionless effective field theory," Phys. Rev. C **72** (2005) 024006, [arXiv:nucl-th/0412002].

[31] M. Creutz, "Transfer Matrices and Lattice Fermions at Finite Density," Found. Phys. **30** (2000) 487.

[32] M. Lüscher, "Volume Dependence of the Energy Spectrum in Massive Quantum Field Theories. 1. Stable Particle States," Commun. Math. Phys. **104** (1986) 177.

[33] M. Lüscher, "Volume Dependence of the Energy Spectrum in Massive Quantum Field Theories. 2. Scattering States," Commun. Math. Phys. **105** (1986) 153.

[34] X. Li and C. Liu, "Two Particle States in an Asymmetric Box," Phys. Lett. B **587** (2004) 100, [arXive:hep-lat/0311035].

[35] X. Feng, X. Li and C. Liu, "Two Particle States in an Asymmetric Box and the Elastic Scattering Phases," Phys. Rev. D **70** (2004) 014505, [arXiv:hep-lat/0404001].

[36] K. Rummukainen and S. A. Gottlieb, "Resonance Scattering Phase Shifts on a Non-Rest Frame Lattice," Nucl. Phys. B **450** (1995) 397, [arXiv:hep-lat/9503028].

[37] V. Bernard, M. Lage, U. -G. Meißner and A. Rusetsky, "Resonance properties from the finite-volume energy spectrum," JHEP **0808** (2008) 024, [arXiv:hep-lat/0806.4495].

[38] K. Polejaeva and A. Rusetsky, "Three particles in a finite volume," Eur. Phys. J. A **48** (2012) 67, [arXiv:hep-lat/1203.1241].

[39] S. R. Beane, P. F. Bedaque, A. Parreno and M. J. Savage, "Two Nucleons on a Lattice," Phys. Lett. B **585** (2004) 106, [arXiv:hep-lat/0312004].

[40] A. J. Leggett, "Cooper pairing in spin-polarized Fermi systems," J. Phys. Colloques **41** (1980) 7.

[41] E. Braaten and H. -W. Hammer, "Universality in Few-body Systems with Large Scattering Length," Phys. Rep. **428** (2006) 259.

[42] V. Efimov, "Energy Levels Arising from Resonant Two-body Forces in a Three-body System," Phys. Lett. B **33** (1970) 563.

[43] C. J. Pethick and D. G. Ravenhall, "Matter at Large Neutron Excess and the Physics of Neutron-Star Crusts," Ann. Rev. Nucl. Part. Sci. **45** (1995) 429.

[44] M. H. Anderson, J. R. Ensher, M. R. Matthews, C. E. Wieman and E. A. Cornell, "Observation of Bose-Einstein Condensation in a Dilute Atomic Vapo" Science **269**, (1995) 198.

[45] K. B. Davis, M. O. Mewes, M. R. Andrews, N. J. van Druten, D. S. Durfee, D. M. Kurn and W. Ketterle, "Bose-Einstein Condensation in a Gas of Sodium Atoms," Phys. Rev. Lett. **75** (1995) 3969.

[46] C. Regal and D. S. Jin, "Experimental realization of BCS-BEC crossover physics with a Fermi gas of atoms," [arXiv:cond-mat/0601054].

[47] M. Randeria, "Ultracold Fermi gases: Pre-pairing for condensation," Nature Physics **6** (2010) 561-562.

[48] S. Bour, X. Li, D. Lee, U. -G. Meißner and L. Mitas, "Precision benchmark calculations for four particles at unitarity," Phys. Rev. A **83** (2011) 063619, [arXiv:cond-mat.quant-gas/1104.2102].

[49] K. M. O'Hara, S. L. Hemmer, M. E. Gehm, S. R. Granade and J. E. Thomas, "Observation of a Strongly Interacting Degenerate Fermi Gas of Atoms," Science **298** (2002) 2179.

[50] M. Bartenstein, A. Altmeyer, S. Riedl, S. Jochim, C. Chin, J. Denschlag and R. Grimm, "Crossover from a Molecular Bose-Einstein Condensate to a Degenerate Fermi Gas," Phys. Rev. Lett. **92** (2004) 120401, [arXive:cond-mat/0401109v2].

[51] J. Kinast, A. Turlapov, J. E. Thomas, Q. Chen, J. Stajic and K. Levin, "Heat Capacity of a Strongly-Interacting Fermi Gas," Science **307** (2005) 1296, [arXiv:cond-mat/0502087].

[52] L. Luo, J. E. Thomas "Thermodynamic Measurements in a Strongly Interacting Fermi Gas," Journal of Low Temperature Physics **154** (2009) 1, [arXiv:cond-mat.other/0811.1159].

[53] L. Tarruell, M. Teichmann, J. Mckeever, T. Bourdel, J. Cubizolles, L. Khaykovich, J. Zhang, N. Navon, F. Chevy and C. Salomon, "Ultra-Cold Fermi Gases: Proceedings of the International School of Physics "Enrico Fermi", Course CLXIV (I O S Press, Incorporated, 2008)," [arXiv:cond-mat/0701181].

[54] T. Bourdel, L. Khaykovich, J. Cubizolles, J. Zhang, F. Chevy, M. Teichmann, L. Tarruell, S. J. Kokkelmans C. and Salomon, "Experimental Study of the BEC-BCS Crossover Region in Lithium 6," Phys. Rev. Lett. **93** (2004) 050401, [cond-mat/0403091v3]

[55] J. T. Stewart, J. P. Gaebler, C. A. Regal and D. S. Jin, "Potential Energy of a ^{40}K Fermi Gas in the BCS-BEC Crossover," Phys. Rev. Lett. **97** (2006) 220406, [cond-mat/0607776].

[56] J. Joseph, B. Clancy, L. Luo, J. Kinast, A. Turlapov and J. E. Thomas, "Measurement of Sound Velocity in a Fermi Gas near a Feshbach Resonance," Phys. Rev. Lett. **98** (2007) 170401, [cond-mat/0612567v1].

[57] S. NascimbÃĺne1, N. Navon, K. J. Jiang, F. Chevy and C. Salomon "Exploring the thermodynamics of a universal Fermi gas," Nature **463** (2010) 1057.

[58] G. B. Partridge, W. Li, R. I. Kamar, Y. Liao, and R. G. Hulet, "Pairing and Phase Separation in a Polarized Fermi Gas," Science **311** (2006) 503, [arXiv:cond-mat/0511752].

[59] H. Heiselberg, "Fermi systems with long scattering lengths," Phys. Rev. A **63** (2001) 043606.

[60] G. A. Baker, "Neutron matter model," Phys. Rev. C **60** (1999) 054311.

[61] A. Perali, P. Pieri and G. C. Strinati, "Quantitative Comparison between Theoretical Predictions and Experimental Results for the BCS-BEC Crossover," Phys. Rev. Lett. **93** (2004) 100404.

[62] H. Hu, P. D. Drummond and X. -J. Liu "Universal thermodynamics of strongly interacting Fermi gases," Nature Physics **3** (2007) 469, [arXiv:cond-mat/0701744].

[63] S. K. Adhikari "BCS-BEC crossover in a trapped Fermi super-fluid using a density-functional equation," J. Phys. B **43** (2010) 085304, [arXiv:cond-mat.quant-gas/1003.1712].

[64] Y. Nishida and D. T. Son, "ϵ Expansion for a Fermi Gas at Infinite Scattering Length," Phys. Rev. Lett. **97** (2006) 050403.

[65] T. Papenbrock, "Density-functional theory for fermions in the unitary regime," Phys. Rev. A **72** (2005) 041603.

[66] B. Krippa, "Exact renormalisation group flow for ultracold Fermi gases in unitary limit," J. Phys. A **42** (2009) 465002, [arXiv:cond-mat.supr-con/0704.3984].

[67] M. Y. Veillette, D. E. Sheehy and L.Radzihovsky, "Large-N expansion for unitary superfluid Fermi gases," Phys. Rev. A **75** (2007) 043614, [arXiv:cond-mat/0610798].

[68] J. V. Steele, "Effective Field Theory Power Counting at Finite Density," [arXiv:nucl-th/0010066].

[69] J. Carlson and S. Reddy, "Asymmetric Two-component Fermion Systems in Strong Coupling," Phys. Rev. Lett. **95** (2005) 060401, [arXiv:cond-mat/0503256].

[70] E. Burovski, N. Prokof'ev, B. Svistunov and M. Troyer, "Critical Temperature and Thermodynamics of Attractive Fermions at Unitarity," Phys. Rev. Lett. **96** (2006) 160402.

[71] A. Bulgac, J. E. Drut and P. Magierski, "Spin 1/2 Fermions in the Unitary Regime: A Superfluid of a New Type," Phys. Rev. Lett. **96** (2006) 090404.

[72] G. E. Astrakharchik, J. Boronat, J. Casulleras and S. Giorgini, "Equation of State of a Fermi Gas in the BEC-BCS Crossover: A Quantum Monte Carlo Study," Phys. Rev. Lett. **93** (2004) 200404, [arXiv:cond-mat/0406113].

[73] D. Lee, "Ground state energy of spin-1/2 fermions in the unitary limit," Phys. Rev. B **73** (2006) 115112, [arXiv:cond-mat/0511332].

[74] V. K. Akkineni, D. M. Ceperley and N. Trivedi, "Pairing and superfluid properties of dilute fermion gases at unitarity," Phys. Rev. B **76** (2007) 165116,

[75] T. Abe and R. Seki, "From low-density neutron matter to the unitary limit," Phys. Rev. C **79** (2009) 054003, [arXiv:[nucl-th/0708.2524].

[76] D. Lee, "The Symmetric heavy-light ansatz," Eur. Phys. J. A **35** (2008) 171, [arXiv:cond-mat.supr-con/0704.3439].

[77] O. Juillet, "Sign-free stochastic mean-field approach to strongly correlated phases of ultracold fermions," New Journal of Physics **9** (2007) 163, [arXiv:cond-mat/0609063v3].

[78] J. Carlson, S. Y. Chang, V. R. Pandharipande and K. E. Schmidt, "Superfluid Fermi Gases with Large Scattering Length," Phys. Rev. Lett. **91** (2003) 050401.

[79] M. G. Endres, D. B. Kaplan, J. -W. Lee and A. N. Nicholson, "Lattice Monte Carlo calculations for unitary fermions in a finite box," Phys. Rev. A **87** (2013) 023615, [arXiv:hep-lat/203.3169].

[80] K. Rummukainen and S. Gottlieb, "Resonance scattering phase shifts on a non-rest-frame lattice," Nucl. Phys. B **450** (1995) 397.

[81] C. H. Kim, C. T. Sachrajda and S. R. Sharpe, "Finite-volume effects for two-hadron states in moving frames," Nucl. Phys. B **727** (2005) 218.

[82] G. V. Skornyakov and K. A. Ter-Martirosian, Sov. Phys. JETP **4** (1957) 648.

[83] D. S. Petrov, "Three-body problem in Fermi gases with short-range interparticle interaction," Phys. Rev. A **67** (2003) 010703.

[84] D. S Petrov, C. Salomon and G. V. Shlyapnikov, "Scattering properties of weakly bound dimers of fermionic atoms," Phys. Rev. A **71** (2005) 012708.

[85] G. Rupak, "Dimer scattering in the epsilon expansion," [arXiv:nucl-th/0605074].

[86] J. von Stecher, C. H. Greene and D. Blume, "Energetics and structural properties of trapped two-component Fermi gases," Phys. Rev. A **77** (2008) 043619.

[87] A. Rokash, E. Epelbaum, H. Krebs, D. Lee and U. G. Meißner, "Finite volume effects in low-energy neutron-deuteron scattering," J. Phys. **G41** (2013) 015105, [arXive:nucl-th/1308.3386].

[88] J. Levinsen, "Paired fermionic superfluids with s- and p-wave interactions," [arXiv:0807.2840].

[89] J. Levinsen and D. S. Petrov, "Atom-dimer and dimer-dimer scattering in fermionic mixtures near a narrow Feshbach resonance," Eur. Phys. J. D **65** (2011) 67.

[90] F. Chevy and C. Mora, "Ultra-cold polarized Fermi gases," Rep. Prog. Phys. **73** (2010) 112401.

[91] X. Cui and H. Zhai, "Stability of a fully magnetized ferromagnetic state in repulsively interacting ultracold Fermi gases," Phys. Rev. A **81** (2010) 041602.

[92] R. Schmidt and T. Enss, "Excitation spectra and rf response near the polaron-to-molecule transition from the functional renormalization group," Phys. Rev. A **83** (2011) 063620.

[93] P. Massignan and G. M. Bruun, "Repulsive polarons and itinerant ferromagnetism in strongly polarized Fermi gases," Eur. Phys. J. D **65** (2011) 83.

[94] N. Prokov'ev and B. Svistunov, "Fermi-polaron problem: Diagramatic Monte Carlo method for divergent sign-alternating series," Phys. Rev. B **77** (2008) 020408.

[95] R. Combescot and S. Giraud, "Normal State of Highly Polarized Fermi Gases: Full Many-Body Treatment," Phys. Rev. Lett. **101** (2008) 050404.

[96] C. Lobo, A. Recati, S. Giorgini and S. Stringari, "Normal State of a Polarized Fermi Gas at Unitarity," Phys. Rev. Lett. **97** (2006) 200403.

[97] S. Pilati and S. Giorgini, "Phase Separation in a Polarized Fermi Gas at Zero Temperature," Phys. Rev. Lett. **100** (2008) 030401.

[98] F. Chevy, "Universal phase diagram of a strongly interacting Fermi gas with unbalanced spin populations," Phys. Rev A **74** (2006) 063628.

[99] Y. Shin, "Determination of the equation of state of a polarized Fermi gas at unitarity," Phys. Rev. A **77** (2008) 041603.

[100] A. Schirotzek, C. Wu, A. Sommer and M. W. Zwierlein, "Observation of Fermi Polarons in a Tunable Fermi Liquid of Ultracold Atoms," Phys. Rev. Lett. **102** (2009) 230402.

[101] M. M. Forbes, A. Gezerlis, K. Hebeler, T. Lesinski and A. Schwenk, "The neutron polaron as a constraint on nuclear density functionals," [arXiv:nucl-th/1308.1691].

[102] E. Abrahams, "The evolution of high-temperature superconductivity: theory perspective," Int. J. Mod. Phys. B **24** (2010) 4150.

[103] M. M. Parish, "Polaron-molecule transitions in a two-dimensional Fermi gas," Phys. Rev. A **83** (2011) 051603.

[104] S. Zölner, G. M. Bruun and C. J. Pethick, "Polarons and molecules in a two-dimensional Fermi gas," Phys. Rev. A **83** (2011) 021603.

[105] M. Klawunn and A. Recati, "Fermi polaron in two dimensions: Importance of the two-body bound state," Phys. Rev. A **84** (2011) 033607.

[106] R. Schmidt, T. Enss, V. Pietilä and E. Demler, "Fermi polarons in two dimensions," Phys. Rev. A **85** (2012) 021602(R).

[107] B. Fröhlich, M. Feld, E. Vogt, M. Koschorreck, W. Zwerger and M. Köhl, "Radio-Frequency Spectroscopy of a Strongly Interacting Two-Dimensional Fermi Gas," Phys. Rev. Lett. **106** (2011) 105301.

[108] M. Koschorreck, D. Pertot, E. Vogt, B. Fröhlich, M. Feld and M. Köhl, "Attractive and repulsive Fermi polarons in two dimensions," Nature, **480** (2012) 619.

[109] Y. Zhang, W. Ong, I. Arakelyan and J. E. Thomas, "Polaron-to-polaron transitions in the radio-frequency spectrum of a quasi-two-dimensional Fermi gas," Phys. Rev. Lett. **108** (2012) 235302.

[110] E. Vogt, M. Feld, B. Fröhlich, D. Pertot, M. Koschorreck and M. Köhl, "Scale Invariance and Viscosity of a Two-Dimensional Fermi Gas," Phys. Rev. Lett. **108** (2012) 070404.

Chapter 5

Publications

PRECISION BENCHMARK CALCULATIONS FOR FOUR PARTICLES AT UNITARITY

S. Bour, X. Li, D. Lee, U. -G. Meißner and L. Mitas

$\mathcal{PL}$

Phys. Rev. A **83** (2011) 063619

PHYSICAL REVIEW A **83**, 063619 (2011)

Precision benchmark calculations for four particles at unitarity

Shahin Bour,[1] Xin Li,[2] Dean Lee,[2] Ulf-G. Meißner,[1,3] and Lubos Mitas[2]

[1]*Helmholtz-Institut für Strahlen- und Kernphysik (Theorie) and Bethe Center for Theoretical Physics, Universität Bonn, D-53115 Bonn, Germany*

[2]*Department of Physics, North Carolina State University, Raleigh, North Carolina 27695, USA*

[3]*Institut für Kernphysik (IKP-3), Institute for Advanced Simulation (IAS-4), and Jülich Center for Hadron Physics, Forschungszentrum Jülich, D-52425 Jülich, Germany*

(Received 19 April 2011; published 15 June 2011)

The unitarity limit describes interacting particles where the range of the interaction is zero and the scattering length is infinite. We present precision benchmark calculations for two-component fermions at unitarity using three different *ab initio* methods: Hamiltonian lattice formalism using iterated eigenvector methods, Euclidean lattice formalism with auxiliary-field projection Monte Carlo methods, and continuum diffusion Monte Carlo methods with fixed and released nodes. We have calculated the ground-state energy of the unpolarized four-particle system in a periodic cube as a dimensionless fraction of the ground-state energy for the noninteracting system. We obtain values of 0.211(2) and 0.210(2) using two different Hamiltonian lattice representations, 0.206(9) using Euclidean lattice formalism, and an upper bound of 0.212(2) from fixed-node diffusion Monte Carlo methods. Released-node calculations starting from the fixed-node result yield a decrease of less than 0.002 over a propagation of $0.4E_F^{-1}$ in Euclidean time, where E_F is the Fermi energy. We find good agreement among all three *ab initio* methods.

TOPOLOGICAL PHASES
FOR
BOUND STATES MOVING IN A FINITE VOLUME

S. Bour, S. König, D. Lee, H. -W. Hammer and U. -G. Meißner

$\mathcal{PL}$

Phys. Rev. D **84** (2011) 091503

PHYSICAL REVIEW D **84,** 091503(R) (2011)

Topological phases for bound states moving in a finite volume

Shahin Bour,[1] Sebastian König,[1] Dean Lee,[2] H.-W. Hammer,[1] and Ulf-G. Meißner[1,3]

[1]*Helmholtz-Institut für Strahlen- und Kernphysik (Theorie) and Bethe Center for Theoretical Physics, Universität Bonn, 53115 Bonn, Germany*

[2]*Department of Physics, North Carolina State University, Raleigh, North Carolina 27695, USA*

[3]*Institut für Kernphysik, Institute for Advanced Simulation and Jülich Center for Hadron Physics, Forschungszentrum Jülich, D-52425 Jülich, Germany*

(Received 14 July 2011; revised manuscript received 18 October 2011; published 28 November 2011)

We show that bound states moving in a finite periodic volume have an energy correction which is topological in origin and universal in character. The topological volume corrections contain information about the number and mass of the constituents of the bound states. These results have broad applications to lattice calculations involving nucleons, nuclei, hadronic molecules, and cold atoms. We illustrate and verify the analytical results with several numerical lattice calculations.

BENCHMARK CALCULATION
FOR
ELASTIC FERMION-DIMER SCATTERING

S. Bour, H. -W. Hammer, D. Lee and U. -G. Meißner

$\mathcal{PL}$

Phys. Rev. C **86** (2012) 034003

PHYSICAL REVIEW C **86**, 034003 (2012)

Benchmark calculations for elastic fermion-dimer scattering

Shahin Bour,[1] H.-W. Hammer,[1] Dean Lee,[2] and Ulf-G. Meißner[1,3]

[1]*Helmholtz-Institut für Strahlen- und Kernphysik and Bethe Center for Theoretical Physics, Universität Bonn, D-53115 Bonn, Germany*

[2]*Department of Physics, North Carolina State University, Raleigh, North Carolina 27695, USA*

[3]*Institut für Kernphysik, Institute for Advanced Simulation, JARA-HPC and Jülich Center for Hadron Physics, Forschungszentrum Jülich, D-52425 Jülich, Germany*

(Received 18 June 2012; revised manuscript received 22 August 2012; published 14 September 2012)

We present continuum and lattice calculations for elastic scattering between a fermion and a bound dimer in the shallow binding limit. For the lattice calculation we use the finite-volume method of Lüscher. We take into account topological finite-volume corrections to the dimer binding energy which depend on the momentum of the dimer. After subtracting these effects, we find from the lattice calculation $\kappa a_{fd} = 1.174(9)$ and $\kappa r_{fd} = -0.029(13)$. These results agree well with the continuum values $\kappa a_{fd} = 1.17907(1)$ and $\kappa r_{fd} = -0.0383(3)$ obtained from the STM equation. We discuss applications to cold atomic Fermi gases, deuteron-neutron scattering in the spin-quartet channel, and lattice calculations of scattering for nuclei and hadronic molecules at finite volume.